Competitive Activation of N−C and C−H Bonds of the PNP Framework by Monovalent Rhodium and Iridium

Wei Weng, Chengyun Guo, Claudia Moura, Lin Yang, Bruce M. Foxman, and Oleg V. Ozerov*

Department of Chemistry, Brandeis University, MS 015, 415 South Street, Waltham, Massachusetts 02454

Received May 3, 2005

This work describes how reactions of oxidative addition of N−C and C−H bonds are in competition in the PNP-ligated Rh and Ir complexes. Iridium appears to have a higher preference than Rh for the C−H activation over the N−C activation, and the Ir C−H activated complexes are more kinetically stable than their Rh analogues. A new generation of a diarylamido-based PNP pincer is presented, a "tied" PNP ligand **1c** based on the iminodibenzyl substructure. This ligand is more definitively prearranged for binding to a metal center in a meridional, anionic PNP fashion. As a result, its N−C cleavage reactions (that lead to complexes of anionic PNP) are faster than for the "untied" ligands **1a**,**b**. Structural evidence indicates that the "tied" anionic PNP pincer ligand is bulkier than the "untied" ligands when bearing the same substituents on the donor atoms because of the influence of the conformation of the pincer backbone. The "tied" pincer ligand also allows for the observation of the products of activation of the C−H bonds of the central N−CH_3 group, which are not detected with the "untied" ligands. The N−C oxidative addition reaction with "untied" ligands proceeds in the solid state as well as in solution. A remarkable result is reported where the solid-state N−C oxidative addition reaction displays superior selectivity to the solution reaction. The mechanistic studies are augmented by the investigations of the isotopically labeled (^{2}H and ^{13}C) ligands.

Activation of strong bonds remains one of the central issues in synthetic chemistry. Oxidative addition (OA) to a low-valent transition metal is an attractive way of activation of otherwise unreactive bonds. Carbon−nitrogen bonds are ubiquitous in organic compounds, yet only a handful of reports documenting oxidative addition of N−C bonds exist to date.[1,2] Cleavage of N−C bonds is of importance as a necessary step in hydrodenitrogenation of petroleum.[3] The reverse of OA is reductive elimination (RE). RE of N−C bonds has received a much greater deal of attention than the reverse OA,[4] partly because RE of N−C bonds is a crucial step in aromatic[5] and allylic[6] amination. Selective C−H activation is a coveted target for both organic and inorganic chemists.[7] Studies of well-defined elementary transformations and their microscopic reverses provide information that is vital to the development and improvement of catalytic processes.

In our laboratories we have been interested in the chemistry of the diarylamido-based PNP pincer ligand family **D** (Figure 1).[2,8,9] It is analogous to the various PCP pincers **A**,[10] PNP pincers **B** of Fryzuk et al.,[11,12]

* To whom correspondence should be addressed. E-mail: ozerov@brandeis.edu.

(1) (a) Lin, B. L.; Clough, C. R.; Hillhouse, G. L. *J. Am. Chem. Soc.* **2002**, *124*, 2890. (b) Torrent, M.; Musaev, D. G.; Morokuma, K. *Organometallics* **2000**, *19*, 4402. (c) Tayebani, M.; Gambarotta, S.; Yap, G. *Organometallics* **1998**, *17*, 3639. (d) Bonanno, J. B.; Henry, T. P.; Neithamer, D. R.; Wolczanski, P. T.; Lobkovsky, E. B. *J. Am. Chem. Soc.* **1996**, *118*, 5132. (e) Chan, Y. W.; Renner, M. W.; Balch, A. L. *Organometallics* **1983**, *2*, 1888. (f) Gandelman, M.; Milstein, D. *Chem. Commun.* **2000**, 1603 (g) C=N bond cleavages are more common; see ref 8d for references. (h) An example of Pd-catalyzed C−N cleavage is the deallylation at N; however for neutral compounds it only works when N bears strongly electron-withdrawing groups. For a review, see: Guibe, F. *Tetrahedron* **1998**, *54*, 2967. (i) N−C oxidative addition of ammonium and iminium salts to low-valent late transition metals has been described: Aresta, M.; Quaranta, E.; Dibenedetto, A.; Giannoccaro, P.; Tommasi, I.; Lanfranchi, M.; Tiripicchio, A. *Organometallics* **1997**, *16*, 834.

(2) (a) Ozerov, O. V.; Guo, C.; Papkov, V. A.; Foxman, B. M. *J. Am. Chem. Soc.* **2004**, 126, 4792. (b) Ozerov, O. V.; Guo, C.; Fan, L.; Foxman B. M. *Organometallics* **2004**, *23*, 5573.

(3) Gray, S. D.; Weller, K. J.; Bruck, M. A.; Briggs, P. M.; Wigley, D. E. *J. Am. Chem. Soc.* **1995**, *117*, 10678, and references therein.

(4) (a) Yamashita, M.; Hartwig, J. F. *J. Am. Chem. Soc.* **2004**, *126*, 5344. (b) Yamashita, M.; Cuevas Vicario, J. V.; Hartwig, J. F. *J. Am. Chem. Soc.* **2003**, *125*, 16347. (c) Hartwig, J. F. *Angew. Chem., Int. Ed.* **1998**, *37*, 2090. (d) Mann, G.; Hartwig, J. F.; Driver, M. S.; Fernandez-Rivas, C. *J. Am. Chem. Soc.* **1998**, *120*, 827. (e) Driver, M. S.; Hartwig, J. F. *J. Am. Chem. Soc.* **1997**, *119*, 8232. (f) Driver, M. S.; Hartwig, J. F. *J. Am. Chem. Soc.* **1996**, *118*, 7217. (g) Hartwig, J. F.; Richards, S.; Baranano, D.; Paul, F. *J. Am. Chem. Soc.* **1996**, *118*, 3626. (h) Widenhoefer, R. A.; Buchwald, S. L. *Organometallics* **1996**, *15*, 3534. (i) Villanueva, L. A.; Abboud, K. A.; Boncella, J. M. *Organometallics* **1994**, *13*, 3921.

(5) (a) Hartwig, J. F. *Synlett* **1997**, 329. (b) Hartwig, J. F. *Acc. Chem. Res.* **1998**, *31*, 852. (c) Hartwig, J. F. *Angew. Chem., Int. Ed.* **1998**, *37*, 2046. (d) Wolfe, J. P.; Wagaw, S.; Marcoux, J.-F.; Buchwald, S. L. *Acc. Chem. Res.* **1998**, *31*, 805. (e) Hartwig, J. F. In *Modern Amination Methods*; Ricci, A., Ed.; Wiley-VCH: Weinheim, 2000; p 195. (f) Muci, A. R.; Buchwald, S. L. *Top. Curr. Chem.* **2001**, *219*, 131.

(6) (a) Trost, B. M. *Chem. Pharm. Bull.* **2002**, *50*, 1. (b) Johannsen, M.; Jørgensen, K. A. *Chem. Rev.* **1998**, *98*, 1689.

(7) (a) Crabtree, R. H. *Chem. Rev.* **1995**, *95*, 987. (b) Arndtsen, B. A.; Bergman, R. G.; Mobley, T. A.; Peterson, T. H. *Acc. Chem. Res.* **1995**, *28*, 154. (c) Shilov, A. E.; Shulpin, G. B. *Chem. Rev.* **1997**, *97*, 2879. (d) Stahl, S.; Labinger, J. A.; Bercaw, J. E. *Angew. Chem., Int. Ed.* **1998**, *37*, 2181. (e) Shilov, A. E.; Shulpin, G. B. *Activation and Catalytic Reactions of Saturated Hydrocarbons in the Presence of Metal Complexes*; Kluwer: Boston, MA, 2000. (f) Crabtree, R. H. *J. Chem. Soc., Dalton Trans.* **2001**, 2437. (g) Jia, C.; Kitamura, T.; Fujiwara, Y. *Acc. Chem. Res.* **2001**, *34*, 633. (h) Labinger, J. A.; Bercaw, J. E. *Nature* **2002**, *417*, 507.

10.1021/om050346o CCC: $30.25 © 2005 American Chemical Society
Publication on Web 06/10/2005

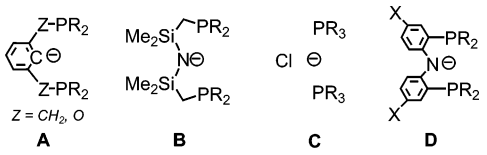

Figure 1.

and the widespread *mer*-Cl(PR_3)$_2$ motif (**C**). We have shown that the N−C bond in ligands **1a** and **1b** can be easily cleaved via OA to several late transition metals.[2] In the context of group 9 metals, we have only characterized activation of the N−C bond in **1a** prior to this work.[2a] In the present report we detail how changes in the properties of the PNP pincer ligand affect the balance among concomitant OA of N−C and of two different types of C−H bonds to monovalent Rh and Ir. Both the N−C and especially the C−H activation are topics of heightened interest.[1−7] C−H activation of amines and N-containing compounds has received special attention recently.[13] We have previously speculated[2a] that the N−C cleavage reactions are driven by the predisposition of the PNP backbone to bind to the metal as an anionic, meridional ligand. To this end, we are now reporting a new PNP ligand, **1c** (and its precursor **1d**), with enhanced such predisposition and its reactions. We will refer to the ligands where the two aryl rings are tied together by a CH_2CH_2 tether as "tied" PNP ligands. The present work also includes a remarkable account of how the selectivity of the reaction of **1b** with Rh^I is altered by performing the reaction in the solid state.

Our work on N−C and C−H OA in PNP pincer ligands is closely related to and indeed inspired by the investigations of C−C and C−H OA reactions in the PCP system by Milstein et al.[10] Other relevant studies from the same group include the C−O OA chemistry.[14]

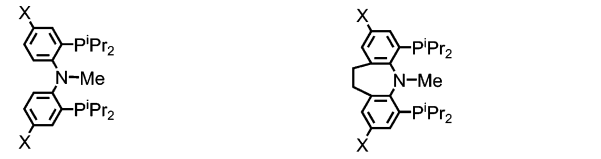

^{Me}PN(Me)P (**1a**): X= CH_3, Me = CH_3
^{Me}PN($^{13}CH_3$)P (**1a-*^{13}C***): X = CH_3, Me = CH_3
^{Me}PN(CD_3)P (**1a-*d_3***): X = CH_3, Me = CD_3

^{F}PNP (**1b**): X= F, Me = CH_3

THPN(Me)P (**1c**): X= H, Me = CH_3
THPN($^{13}CH_3$)P (**1c-*^{13}C***): X= H, Me = $^{13}CH_3$
THPN(CD_3)P (**1c-*d_3***): X = H, Me = CD_3

^{TBr}PN(Me)P (**1d**): X= Br, Me = CH_3
^{TBr}PN($^{13}CH_3$)P (**1d-*^{13}C***): X= Br, Me = $^{13}CH_3$
^{TBr}PN(CD_3)P (**1d-*d_3***): X = Br, Me = CD_3

Figure 2.

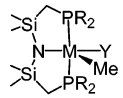

2 *M = Rh, Ir; Y = Br, I;*

Figure 3.

Scheme 1

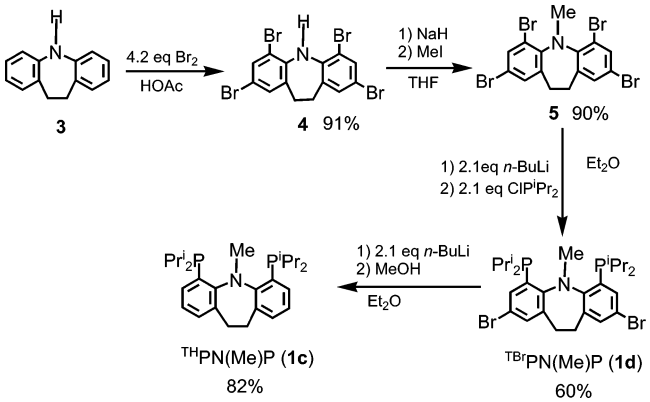

An early indication that the N−C OA to Rh^I and Ir^I in PNP-based systems is likely to be favorable comes from the work of Fryzuk et al.[11] Fryzuk's complexes **2** (Figure 3) were not prepared via OA of N−C, but they are thermally stable, i.e., do not undergo reductive elimination (RE) of N−C.[15]

Results and Discussion

Preparation and Characterization of the Ligands. We have adapted the methodology used previously for the synthesis of **1a** and **1b** to the new PNP ligands **1c** and **1d** (Scheme 1).[2a,8d] Bromination of **3** provides **4** selectively in high yield. *N*-Methylation of **4** by using sodium hydride and methyl iodide furnishes **5** in 90% yield. The lithium−bromine exchange in **5** is selective for the *ortho*-position (similarly to other related examples),[8d,16] and subsequent addition of $ClPPr^i_2$ produces **1d**. Further lithium−bromine exchange followed by protolysis affords **1c**. Compound **1d** is formed in >90% yield and purity in situ (NMR evidence), but its

(8) (a) Bailey, B. C.; Huffman, J. C.; Mindiola, D. J.; Weng, W.; Ozerov, O. V. *Organometallics* **2005**, *24*, 1390. (b) Çelenligil-Çetin, R.; Watson, L. A.; Guo, C.; Foxman, B. M.; Ozerov, O. V. *Organometallics* **2005**, *24*, 186. (c) Weng, W.; Yang, L.; Foxman, B. M.; Ozerov, O. V. *Organometallics* **2004**, *23*, 4700. (d) Fan, L.; Yang, L.; Guo, C.; Foxman, B. M.; Ozerov, O. V. *Organometallics* **2004**, *23*, 4778. (e) Fan, L.; Foxman, B. M.; Ozerov, O. V. *Organometallics* **2004**, *23*, 326.

(9) (a) Liang, L.-C.; Lin, J.-M.; Hung, C.-H. *Organometallics* **2003**, *22*, 3007. (b) Huang, M.-H.; Liang, L.-C. *Organometallics* **2004**, *23*, 2813. (c) Winter, A. M.; Eichele, K.; Mack, H.-G.; Potuznik, S.; Mayer, H. A.; Kaska, W. C. *J. Organomet. Chem*. **2003**, *682*, 149. (d) Harkins, S. B.; Peters, J. C. *J. Am. Chem. Soc*. **2005**, *127*, 2030.

(10) (a) Moulton, C. J.; Shaw, B. L. *J. Chem. Soc., Dalton Trans*. **1976**, 1020. (b) van der Boom, M. E.; Milstein, D. *Chem. Rev*. **2003**, *103*, 1759. (c) Rybtchinski, B.; Vigalok, A.; Ben-David, Y.; Milstein, D. *J. Am. Chem. Soc*. **1996**, *118*, 12406. (d) Liou, S.-Y.; Gozin, M.; Milstein, D. *J. Am. Chem. Soc*. **1995**, *117*, 9774. (e) Sundermann, A.; Uzan, O.; Milstein, D.; Martin, J. M. L. *J. Am. Chem. Soc*. **2000**, *122*, 7095.

(11) (a) Fryzuk, M. D. *Can. J. Chem*. **1992**, *70*, 2839−2845. (b) Fryzuk, M. D.; Berg, D. J.; Haddad, T. S. *Coord. Chem. Rev*. **1990**, *99*, 137. (c) Fryzuk, M. D.; Montgomery, C. D. *Coord. Chem. Rev*. **1989**, *95*, 1. (d) Fryzuk, Michael D.; MacNeil, P. A. *J. Am. Chem. Soc*. **1984**, *106*, 6993. (e) Fryzuk, M. D.; Macneil, P. A.; Rettig, S. J.; Secco, A. S.; Trotter, J. *Organometallics* **1982**, *1*, 918−930.

(12) For Re chemistry with the Fryzuk ligand see: Ozerov, O. V.; Huffman, J. C.; Watson, L. A.; Caulton, K. G. *J. Am. Chem. Soc*. **2004**, *126*, 6363, and references within.

(13) (a) Wang, X.; Lane, B. S.; Sames, D. *J. Am. Chem. Soc*. **2005**, *127*, 4996−4997. (b) Giri, R.; Chen, X.; Yu, J.-Q. *Angew. Chem., Int. Ed*. **2005**, *44*, 1112. (c) Ozerov, O. V.; Pink, M.; Watson, L. A.; Caulton, K. G. *J. Am. Chem. Soc*. **2004**, *126*, 2105. (d) Desai, L. V.; Hull, K. L.; Sanford, M. S. *J. Am. Chem. Soc*. **2004**, *126*, 9542. (e) Dick, A. R.; Hull, K. L.; Sanford, M. S. *J. Am. Chem. Soc*. **2004**, *126*, 2300. (f) Sezen, B.; Sames, D. *J. Am. Chem. Soc*. **2004**, *126*, 13244. (g) Lane, B. S.; Sames, D. *Org. Lett*. **2004**, *6*, 2897. (h) Zhang, X.; Fried, A.; Knapp, S.; Goldman, A. S. *Chem. Commun*. **2003**, *16*, 2060. (i) Ferrando-Miguel, G.; Coalter, J. N., III; Gerard, H.; Huffman, J. C.; Eisenstein, O.; Caulton, K. G. *New J. Chem*. **2002**, *26*, 687.

(14) (a) van der Boom, M. E.; Liou, S.-Y.; Ben-David, Y.; Vigalok, A.; Milstein, D. *Angew. Chem., Int. Ed. Engl*. **1997**, *36*, 625. (b) van der Boom, M. E.; Liou, S.-Y.; Ben-David, Y.; Shimon, L. J. W.; Milstein, D. *J. Am. Chem. Soc.* **1998**, *120*, 6531.

(15) (a) Fryzuk, M. D.; MacNeil, P. A.; Rettig, S. J. *J. Am. Chem. Soc*. **1987**, *109*, 2803. (b) Fryzuk, M. D.; MacNeil, P. A.; Rettig, S. J. *Organometallics* **1986**, *5*, 2469. (d) Fryzuk, M. D.; MacNeil, P. A.; Rettig, S. J. *Organometallics* **1985**, *4*, 1145.

(16) Wasserman, D.; Jones, R. E.; Robinson, S. A.; Garber, J. D. *J. Org. Chem*. **1965**, *30*, 3248.

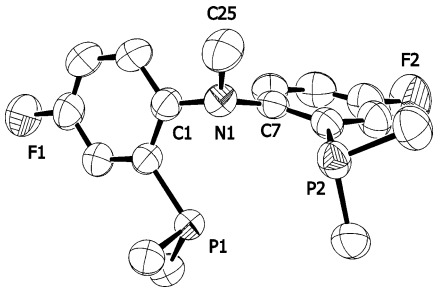

Figure 4. ORTEP drawing (50% probability ellipsoids) of **1b** showing selected atom labeling.[17] Omitted for clarity: H atoms, methyls of the ^{i}Pr groups. Selected bond distances (Å) and angles (deg) follow: C27−N1, 1.429 (3), C7−N1−C1, 116.86(7), C1−N1−C25, 114.80(18), C7−N1−C25, 112.83(18).

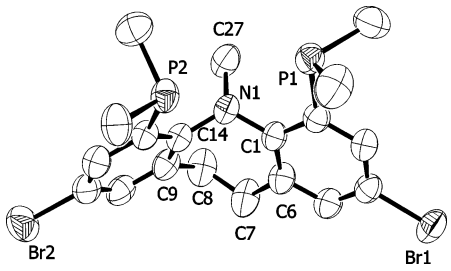

Figure 5. ORTEP drawing (50% probability ellipsoids) of **1d** showing selected atom labeling.[17] Omitted for clarity: H atoms, methyls of the ^{i}Pr groups. Selected bond distances (Å) and angles (deg) follow: C27−N1, 1.463 (6), C27−N1−C1, 116.3(3), C27−N1−C14, 116.7(3), C1−N1−C14, 119.6(3).

high lipophilicity hampers its isolation. As a result, we have been able to obtain pure, solid **1d** only in 60% isolated yield. Preparation of the isotopically labeled **1c-*d*$_3$**, **1c-*^{13}C***, **1d-*d*$_3$**, and **1d-*^{13}C*** was carried out analogously, using CD_3I or $^{13}CH_3I$ in place of the natural abundance CH_3I. Overall, the synthesis of **1c/1d** is perhaps more economical than that of **1a/1b** and the like because of the commercial availability of the inexpensive iminodibenzyl **3** (ca. $0.4/g). In contrast, bis(*p*-tolyl)amine and bis(*p*-fluorophenyl)amine precursors for **1a** and **1b** are more expensive or have to be synthesized using the Pd-catalyzed amination protocol.[5,8d,e]

Compounds **1c/1d** and **3**−**5** have been fully characterized by NMR in solution. **3** and **4** display C_{2v} symmetry, while **5**, **1c**, and **1d** display C_s symmetry on the NMR time scale. The ^{1}H NMR resonances of the CH_2-CH_2 linker are particularly telling. These four hydrogens give rise to a singlet in **3** and **4**, but to a pair of multiplets for **5**, **1c**, and **1d** (geminal $J_{H-H} \approx 16$ Hz). The iminodibenzyl unit ideally should possess time-averaged C_{2v} symmetry. The time averaging is apparently fast for **3** and **4** (central NH group), but not for **5**, **1c**, and **1d** with a central N−Me moiety. The flip-flopping motion that results in the time-averaged C_{2v} symmetry necessitates that the central NH or NMe group travel between "above" and "below" the average plane of iminodibenzyl. Such motion should be impeded for NMe because the alignment of NMe with the two *ortho*-substituents in the same plane (presumably the transition state for the flip) is greatly disvafored for steric reasons. This view is supported by the solid-state structures of **1b** and **1d** (Figures 4 and 5). In **1d**, the N-bound methyl group is markedly pointed away from the centroid of the P−P line and the overall structure is strongly *puckered* (the angle between the two aromatic rings is ca. 54°; the C6−C7−C8−C9 torsion angle is ca. 67°). The symmetry of the solid-state structure is C_1. Without the passing of the Me group between the two P atoms the conformational motions of the molecule can bring the time-averaged symmetry only to C_s.

On the other hand, in the solid-state structure of **1b**, the two aromatic rings are nearly perpendicular to each other (the interplanar angle is ca. 94°). The diarylamine system is rather *twisted* than puckered in **1b**. It is clear that the solid-state conformation of **1b** is unattainable for **1d**. The distance between the two phosphorus atoms of the same molecule in the solid-state structure of **1b** is 4.145(1) Å, while it is much shorter in that of **1d** (3.721(2) Å). This demonstrates that the P, N, P donors are held more rigidly in place in the "tied" ligand. The smaller inter-phosphorus distance for **1d** is also consistent with the apparent inability of the Me group to pass through the PNP plane rapidly on the NMR time scale, in contrast to **1b**. Most likely, this analysis also applies to **1c** (similar to **1d**) and **1a** (similar to **1b**). It is also worth noting that in the structures of both **1b** and **1d** the environment about N is decidedly nonplanar. The sum of angles about N in **1b** is 344.5(3)° and it is 352.6(5)° in **1d**.

The ^{31}P nuclei in each of **1c** and **1d** are equivalent and give rise to ^{31}P NMR resonances at δ −8.8 and −7.7 ppm, respectively. The ^{13}C NMR resonance of N−Me displays coupling to ^{31}P (**1c**: δ 51.3 ppm, t, $J_{P-C} = 10$ Hz; **1d**: δ 50.9 ppm, t, $J_{P-C} = 10$ Hz), while the ^{1}H NMR resonance of the N−Me group is a singlet (**1c**: 3.46 ppm; **1d**: δ 3.25 ppm). These data are similar to those for the previously reported PN(Me)P ligands.[2,8]

The ^{13}C-labeled compounds **5-*^{13}C***, **1c-*^{13}C***, and **1d-*^{13}C*** display the appropriate ^{31}P−^{13}C and ^{1}H−^{13}C coupling in their ^{31}P NMR (**5-*^{13}C***: $J_{P-C} = 9$ Hz, **1c-*^{13}C*** and **1-*^{13}C***: $J_{P-C} = 10$ Hz) and ^{1}H NMR spectra (**5-*^{13}C***, **1c-*^{13}C***, and **1d-*^{13}C***: $^1J_{C-H} = 136$ Hz), respectively. The ^{2}H resonances arising from N−CD_3 of **1d-*d*$_3$** and **1c-*d*$_3$** are at δ 3.16 and 3.37 ppm, respectively.

N−C Cleavage with Pd^{II}. Upon design, we believed that the "tied" ligand **1c** should be more strongly prearranged to give rise to anionic *mer*-PNP complexes and that the backbone of such ligands should be closer to planarity. To test these assumptions, we prepared (THPNP)PdCl (**6c**), closely analogous to (^{Me}PNP)PdCl (**6a**) that we described in an earlier publication.[8e] (THPNP)PdCl (**6**) was prepared via N−C cleavage from **1c** and (COD)$PdCl_2$ in high yield. We published an extensive investigation of the related N−C cleavage with Pd^{II} elsewhere.[8d] The solid-state structure of **6c** (Figures 6, 7) was established with the help of an X-ray diffraction study performed on a suitable single crystal. Although the Pd chemistry of PNP is outside the scope of this report, the comparison between the structural parameters in **6c** and **6a** gives a quantitative measure of the intrinsic differences between the "tied" and the "untied" PNP ligands (Table 1). The structure of **6c** is indeed "more planar": the angle between the two aromatic rings and the angle between the coordination planes of N and Pd are smaller in **6c** than in **6a**. A consequence of this flattening is that the phosphine donors in **6c** are pushed farther toward Cl and also

Table 1. Comparative Geometrical Parameters in 6a and 6c

	(^{Me}PNP)PdCl (**6a**)	(THPNP)PdCl (**6c**)
ring/ring angle	ca. 46°	ca. 33°
N/Pd planes angle	ca. 29°	ca. 20°
P−Pd−P angle	163.54(2)°	169.95(5)°
Pd−P distance	2.2914(4) Å	2.2643(13) Å 2.2504(13) Å
N−Pd distance	2.0258(19) Å	2.068(4) Å
Pd−Cl distance	2.3157(7) Å	2.3165(15) Å
P···P distance	4.535(1) Å	4.497(2) Å

Scheme 2

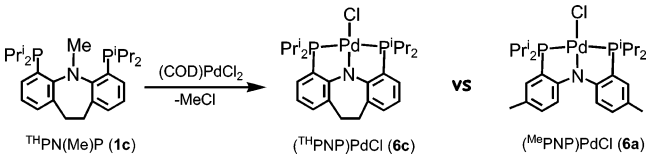

closer to the metal: the P−Pd−P angle is greater while the Pd−P distances are shorter in **6c**. These features make the "tied" pincer effectively bulkier than the "untied" ligands without changing the nature of the substituents on P, a subtle but potentially useful effect. The Pd−N bond is longer in **6c**, but this is intuitively consistent with the overall distortion. The longer Pd−N distance should make the amido donor in **6c** a weaker trans-influence ligand than that in **6a**, but the two Pd−Cl distances (trans to N) in **6c** and **6a** are essentially identical. It is plausible that the weakened trans-influence of N (expect shortening of Pd−Cl) is counteracted by the increase in the steric pressure from the P donors (expect elongation of Pd−Cl). Interestingly, the separation between the two P atoms in **6c** is actually ca. 0.77 Å greater than that in the free ligand **1d** (and presumably **1c**). In effect, the metal center has to push the phosphine arms apart to fit in (this is also consistent with the shorter Pd−P bonds in **6c** vs **6a**). The strain of such distortion is "absorbed" by the CH_2CH_2 linker as the C6−C7−C8−C9 dihedral angle increases from ca. 67° in **1d** to ca. 88° in **6c**.

The solution symmetry of **6c** by NMR at ambient temperature is C_{2v}. This indicates that replacing the Me in **1c**(**1d**) with a PdCl fragment (which, unlike Me in **1d**, is always in the PNP plane) facilitates the flip-flop of the PNP ligand backbone.

Reactions of 1a−c with Rh^{I}. We previously reported that **1a** reacts with $[Rh(COD)Cl]_2$ with eventual near-quantitative conversion to the N−C oxidative addition product **8a** (Scheme 3).[2a] Intermediate **7a** was detected and could be isolated. **7a** transforms into **8a** in a clean first-order reaction with $t_{1/2}$(298 K) of ca. 13 h.[2a] We were interested to examine how this reaction is affected by changes in the electronic and the geometric properties of the ligand. Ligand **1b** serves as an example of a less donating PNP ligand. In addition, ^{19}F NMR is an excellent probe for detection of small concentrations of products in solution. Ligand **1c** is apparently similar to **1a** electronically: each has one alkyl substituent per aromatic ring of the backbone and the same substituents on P. However, we view **1c** as more rigidly prearranged for coordination to the metal as a meridional anionic PNP ligand.

Similarly to the reaction with **1a**,[2a] $[(COD)RhCl]_2$ and **1b** in aromatic solvents readily produce the Rh^{I} adduct

Scheme 3

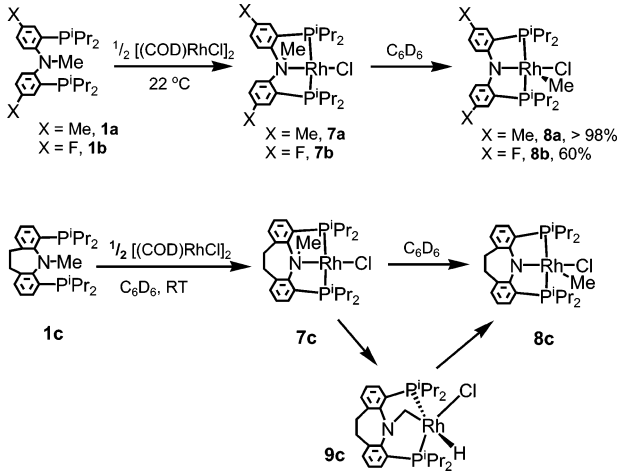

7b within a few minutes of mixing. Upon standing at 22 °C, C_6D_6 solutions of **7b** slowly evolve into a mixture of products. **8b** is a major product; however, several other peaks are evident in the ^{31}P and ^{19}F NMR spectra. Prolonged standing at 22 °C or thermolysis (80 °C) do not lead to conversion to a single product. ^{19}F NMR is a helpful tool in identifying the coordination mode of the ^{F}PNP ligand. From this work and prior work with Ni, Pd, and Pt,[8d] we have identified three general situations distinguishable by ^{19}F NMR: (a) free ligand **1b** resonates at δ −123.2 ppm; (b) metal complexes of the neutral **1b** as ^{F}PN(Me)P resonate downfield of the resonance of free **1b**, in the δ −112 to −118 ppm region; (c) metal complexes of the anionic ^{F}PNP ligand resonate upfield of free **1b**, in the δ −129 to −133 ppm region. The ^{19}F NMR chemical shift is generally reflective of how electron rich the backbone aromatic ring is.[19] In the mixture that evolves from **7b**, the only significant ^{19}F NMR resonance upfield of free **1b** is that of **8b** (δ −130.6 ppm). We have not been able to identify other components of the mixture, but it is possible that they stem from the activation of the surrounding C−H bonds. **8b** was fully characterized by solution NMR methods; its pertinent NMR characteristics are very similar to those of **8a**.[2a]

The reaction between **1c** and $[(COD)RhCl]_2$ (Scheme 3) eventually led exclusively to the N−C oxidative addition product **8c**. At the intermediate stages of the reaction, a mixture of **1c**, **7c**, **8c**, and **9c** was observed that eventually evolved exclusively into **8c** after <7 h at 22 °C (cf. $t_{1/2}(298) = 13$ h for formation of **8a**). We thus conclude that *the utilization of a "tied", more rigid PN(Me)P ligand accelerates N−C cleavage*. We were unable to isolate **7c** or **9c** because the rate of their formation is comparable to the rate of conversion to **8c**, and they were only characterized in solution. The proposed structural identification of **9c** is discussed later in this article in conjunction with the Ir analogue **16c**. Utilization of the ^{13}C-labeled ligand **1c-*^{13}C*** allowed for convenient analysis of this transformation by ^{13}C (Figure 8) and $^{13}C\{^1H\}$ NMR. Compounds **1c** and **7c** display ^{13}C resonances typical of a CH_3 group attached to N.[20]

(17) ORTEP plots were created using Ortep-3 for Windows. Farugia, L. *J. Appl. Crystallogr.* **1997**, *30*, 565.

(18) Persistence of Vision Ray Tracer (POV-Ray), available at http://www.povray.org/.

(19) Hansch, C.; Leo, A.; Taft, R. W. *Chem. Rev.* **1991**, *91*, 165.

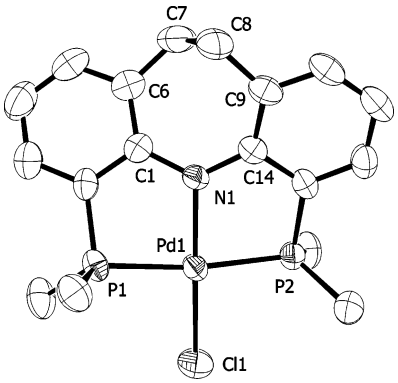

Figure 6. ORTEP drawing (50% probability ellipsoids) of **6c** showing selected atom labeling.[17] Omitted for clarity: H atoms, methyls of the ^{i}Pr groups.

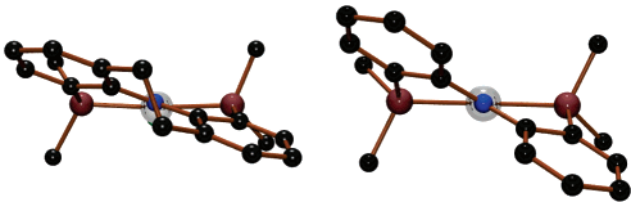

Figure 7. POV-Ray ball-and-stick renditions of the solid-state structures of **6c** (left) and **6a** (right) viewed along the N−Pd−Cl axis.[18] Omitted for clarity: H atoms, methyls of the ^{i}Pr groups and on the aryl rings. Color coding: N, blue; Rh, chrome; C, black; P, brown-red; Cl, green.

On the other hand, the $^{13}CH_3$ signal in **8c** is indicative of a Rh−Me moiety[2a,10c−e] and the $^{13}CH_2$ signal in **9c** is indicative of a N−CH_2−Rh linkage.

The ^{1}H (δ 2.33, dt, J_{HP} = 5 Hz, J_{H-Rh} = 3 Hz) and ^{13}C (δ 3.75, undecoupled, qdt, J_{H-C} = 141 Hz, J_{Rh-C} = 29 Hz, J_{P-C} = 5 Hz) NMR data for the Rh−Me group in **8c** are very similar to those in **8a** and **8b** as is the distinct green color.[2a] The NMR chemical shifts and coupling constants for the ^{13}C and ^{1}H resonances of the Rh−Me group in **8a**−**c** are also similar to those of (PCP)Rh(Me)Cl reported by Milstein et al.[10c,d] In both cases the Me group is trans to the empty site. The ^{31}P{^{1}H} NMR spectrum of **8c**, on the other hand, differs from those of **8a** and **8b**. Two broad signals (δ 42.6 and 36.7 ppm) are evident at 20 °C; they coalesce into one broad singlet (δ 39.7 ppm) at 50 °C. This chemical shift is similar to those recorded for **8a** and **8b**. We believe that the broadness and the nonequivalence of the ^{31}P NMR resonances in **8c** is caused by the slower flip-flopping motion of the PNP backbone in the "tied" ligand in **8c**. This is not observed in **6c**. Evidently, the apical Me group in **8c** is a critical impediment to conformational laxity.

Solid-State Formation of 8b. The extraordinary feature of the **7a** → **8a** N−C oxidative addition is that it also proceeds in the solid state as a crystal-to-crystal reaction.[2a] We were curious whether a similar solid-state reaction would proceed with other PNP ligands. Furthermore, we were interested to investigate whether the selectivity of the solid-state **7b** → **8b** reaction was different from the reaction in solution. The results turned out to be remarkable. **7b** has a sufficiently long lifetime to be isolated in a pure form by crystallization at −35 °C. A sample of **7b** thus obtained was heated under argon at 70 °C for 3 h. A color change to dark green was apparent in the solid state. The resultant solid was dissolved in C_6D_6 without purification. *We were unable to detect even traces of any compounds other than **8b** by ^{1}H, ^{31}P, or ^{19}F NMR*. This is in stark contrast to the complex mixture obtained in the solution reaction (Figure 9). The potential of the solid-state synthesis in organometallic chemistry is probably underestimated despite the available body of encouraging data.[21] Our example here illustrates that the solid-state route may bring about not only changes in rate but also drastic (and desirable!) changes in the selectivity of organometallic reactions. A separate investigation of the factors responsible for the selective formation of **8b** in the solid state is warranted, and we intend to undertake it in due course.

Reactions of 1a−c with Ir^{I}. Mixing of **1a** or **1b** with $[(COD)IrCl]_2$ (PNP:Ir = 1:1) in C_6D_6 results in a rapid formation of yellow material that is only sparingly soluble in C_6D_6 and mostly precipitates out of the solution. Thermolysis of the suspension (80 °C, 3 h) results in the formation of a homogeneous green solution that contains a mixture of **10a**(**10b**) and two isomers of **11a**(**11b**) (Scheme 4).[2a] If an analogous reaction with **1a** is performed in fluorobenzene, the initially formed yellow material is fully soluble and thermolysis leads to the same final products. We have now identified the yellow material as **12a**(**12b**), an ionic compound with a $[(^{Me}PN(Me)P)Ir(COD)]^+$ or $[(^{F}PN(Me)P)Ir(COD)]^+$ cation and a mixture of Cl^- and $[Ir(COD)Cl_2]^-$ anions. Since some of Ir is thus tied up in the form of $[Ir(COD)Cl_2]^-$, the mixture contains a corresponding amount of free **1a** or **1b** ligand. To substantiate the identification, we have independently prepared compounds $[(^{Me}PN(Me)P)Ir(COD)]OTf$ (**12a**), $[(^{Me}PN(Me)P)Ir(COD)]OTf$ (**13b**), and $Bu_4N[(COD)IrCl_2]$ (**14**) (Scheme 5). Figure 10 shows overlaid ^{1}H NMR spectra of **12a**, **13a**, and **14**. It is apparent that two sets of COD signals are found in **12a**.

The coordination of PN(Me)P to the (COD)IrCl fragment does not lead immediately to liberation of free COD, as is the case with Rh, but to loss of Cl^-. The liberated chloride competes with PN(Me)P for coordination to the remaining (COD)IrCl fragments, accounting for the formation of $[Ir(COD)Cl_2]^-$. This competition is apparently of thermodynamic and not kinetic nature. The ratio of $[(PN(Me)P)Ir(COD)]^+$ to free PN(Me)P (**1a** or **1b**) is rapidly (<15 min) established and remains unchanged for several hours at 22 °C. Addition of excess **1b** was found to lead to an increase of the concentration of $[(PN(Me)P)Ir(COD)]^+$ and a decrease of the concentration of $[Ir(COD)Cl_2]^-$ (NMR evidence). Formation of $[L_3Ir(COD)]^+$ cations with tridentate neutral L_3 ligands has been noted by others.[22] The formation of $[(PN(Me)P)Ir(COD)]^+$ with Ir but of (PN(Me)P)RhCl (**7**) with

(20) The ^{13}C resonances of **7c-*^{13}C*** and **7c** (or other compounds) are one and the same. That is, the "^{13}C resonance of **7c**" is the resonance of the ca. 1.1% **7c-*^{13}C*** present in the natural abundance sample of **7c**. For brevity we will use "the ^{13}C resonance of **7c**" regardless of whether the natural abundance sample or the isotopically enriched sample is analyzed.

(21) (a) Coville, N. J.; Cheng, L. *J. Organomet. Chem*. **1998**, *571*, 149. (b) Coville, N. J.; Levendis, D. C. *Eur. J. Inorg. Chem*. **2002**, 3067.

(22) (a) Bianchini, C.; Farnetti, E.; Graziani, M.; Nardin, G.; Vacca, A.; Zanobini, F. *J. Am. Chem. Soc*. **1990**, *112*, 9190. (b) Gull, A. M.; Fanwick, P. E.; Kubiak, C. P. *Organometallics* **1993**, *12*, 2121. (c) Flood, T. C.; Iimura, M.; Perotti, J. M.; Rheingold, A. L.; Concolino, T. E. *Chem. Commun*. **2000**, 1681. (d) Budzelaar, P. H. M.; Blok, A. N. J. *Eur. J. Inorg. Chem*. **2004**, 2385.

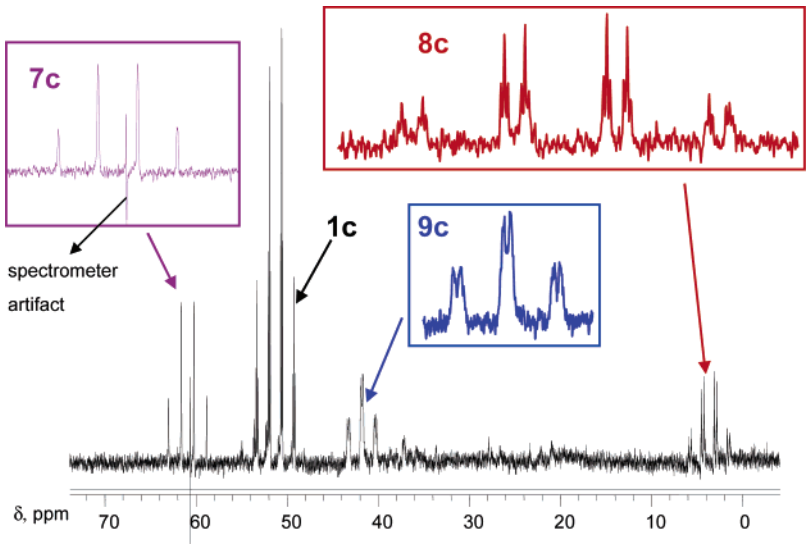

Figure 8. Undecoupled ^{13}C NMR spectrum taken <1 h after mixing **1c-*13C*** and $[(COD)RhCl]_2$ in C_6D_6.

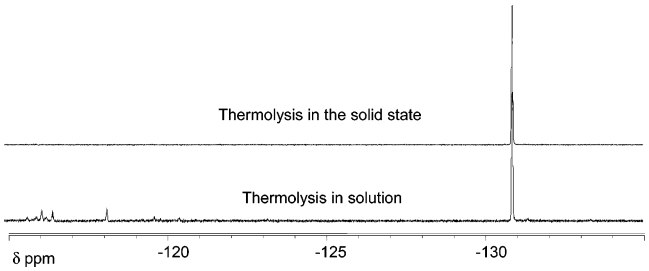

Figure 9. ^{19}F NMR spectra (in C_6D_6) of the mixtures resulting after the thermolysis of **7b** at 70 °C in solution (bottom) and in the solid state (upon dissolution, top).

Rh can be explained by the stronger metal−ligand bonds for Ir, leading to a higher preference for five-coordinate, 18-electron Ir^{I} complexes. The overall conversion to the Ir^{III} products **10** and **11** is much slower than the conversion to the Rh^{III} product **8a**, despite the generally higher preference of the **5d** metal Ir (vs Rh) for higher oxidation states. Clearly, OA reactions are much slower for **12** than they are for **7**. It is possible that the OA of N−C or C−H occurs only via the unobserved intermediate **15**, an Ir analogue of **7** (Scheme 6). If this is the case, then the displacement of COD by Cl^- in $[(PN(Me)P)Ir(COD)]^+$ is the slow step of the overall transformation to Ir^{III} products. $[(PN(Me)P)Ir(COD)]^+$ may be less likely to undergo OA compared to **15** because of the positive charge and the lesser donicity of COD compared to Cl^-. On the other hand, sluggish ligand substitution in $[(PN(Me)P)Ir(COD)]^+$ is easily understood because it is an 18-electron complex with only chelating ligands about Ir.

10a and **10b** could not be isolated in a pure, solid form and were only characterized by NMR in solution. **10a** was previously reported,[2a] and the pertinent NMR data for **10b** are closely analogous. Notably, **10b** resonates in the ^{19}F NMR spectrum (δ −130.8 ppm) at a frequency very similar to its Rh analogue **8b** (δ −130.6 ppm).

The C−H OA product **11a** is formed as a mixture of two isomers (as detected by ^{1}H and ^{31}P NMR). Two easily detectable isomers were also observed for **11b**. Each of the isomers displays two inequivalent ^{31}P NMR resonances with very different chemical shifts ($\Delta\delta$ > 60 ppm). The P−P coupling was not detected (presumably 1 Hz or less), implying cisoid disposition of the two phosphine arms about Ir. That the two P nuclei are bound to the same Ir center is confirmed by the observation of a doublet of doublets for the hydride signals of **11a** and **11b** that resonate at ca. −21 ppm (J_{HP} = 9 Hz, 16 Hz) in the ^{1}H NMR spectrum. Selective decoupling of either of the inequivalent ^{31}P resonances converts the hydride ^{1}H NMR resonance into a doublet. Consistent with their 18-electron count, **11a** and **11b** are air stable in solution and the solid state (unlike the unsaturated **10a** and **10b**). The isomers of **11a** or **11b** do not interconvert during handling. Recrystallization changes the ratio of the isomers, and solutions with persistently different ratios of isomers can thus be obtained. Likewise, **11a** and **10a** (or **11b** and **10b**) do not interconvert at ambient temperature either. Prolonged thermolysis (24 h, 120 °C) of mixtures of **10** and **11** leads to partial decomposition to apparently NMR silent species. **11a** and **11b** are less soluble than **10a** or **10b** and can be isolated by crystallization, at least as mixtures of isomers.

The structural assignment of **11a** was confirmed by an X-ray diffraction study (Figure 11). We cannot be certain whether the crystal selected for the X-ray study represents the major or the minor isomer, but the connectivity is invariant. In the solid-state structure of **11a**, the environment about Ir is strongly distorted from octahedral (expected for Ir^{III}), presumably because of the severe chelate constraints. The hydride was not located, but its presence is unequivocal from the solution NMR data, and it is clear that it occupies a position trans to N. The large difference between the two Ir−P distances likely stems from that Ir−P2 is a part of a four-membered iridacycle. In addition, P2 is trans to Cl, while P1 is trans to an alkyl, a stronger trans influence ligand. Thus, Ir−P2 is predictably shorter.

Reaction of **1c** with $[(COD)IrCl]_2$ initially leads to a yellow material poorly soluble in C_6D_6. We have not investigated its nature but assume it to be similar to **12a**. After 24 h at 22 °C, the solution is green and homogeneous (Scheme 7). Green is the color of **10a** and presumably **10c**. NMR analysis indicated the presence of **10c**, **11c**, and **16c** in a 1:2:1 ratio (along with an adventitious excess of **1c** and a few other unidentified

Scheme 4

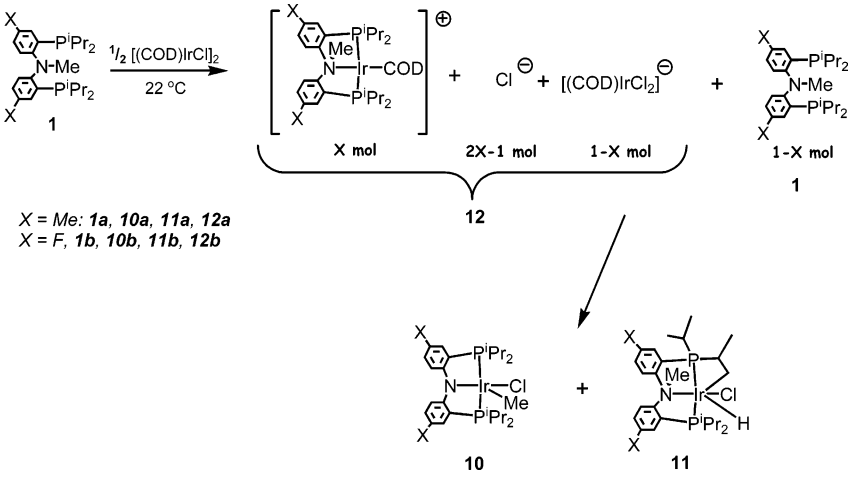

Scheme 5

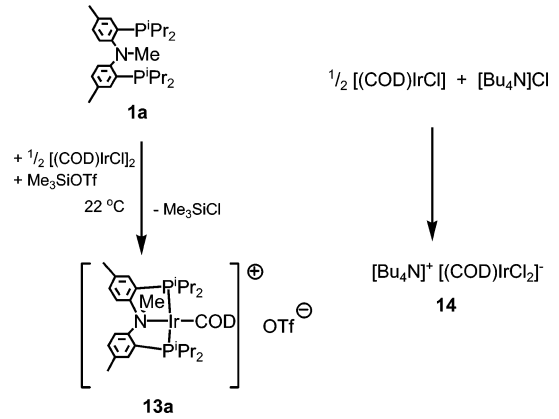

Scheme 6

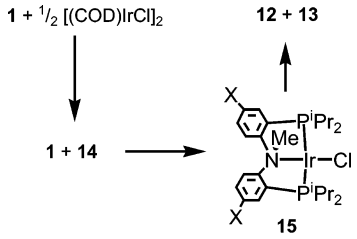

compounds totaling less than 5% of the mixture). As in the Rh case, the transformation to the Ir^{III} products is faster for the "tied" than for the "untied" ligands. Identification was aided by the use of the ^{13}C-labeled ligand **1c-*^{13}C***. The $N-{}^{13}CH_3$, $N-{}^{13}CH_2-Ir$, and $Ir-{}^{13}CH_3$ signals are quite distinct (Figure 12) in the undecoupled ^{13}C NMR spectrum. We have not been able to isolate any of these compounds in the pure form owing to comparable solubility. The NMR spectroscopic features of **11c** (two isomers evident) are similar to those of **11a** and **11b**. The ^{31}P NMR spectrum of **10c**, like its

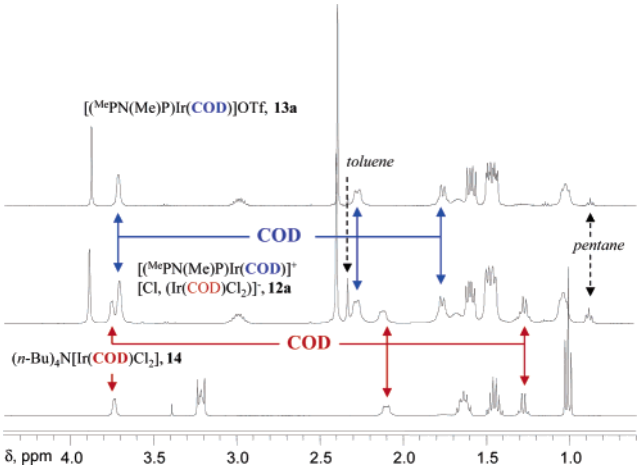

Figure 10. ^1H NMR spectra (in $CDCl_3$) of **12a** (center), **13a** (top), and **14** (bottom).

Rh analogue **8c** (vide supra), displays two very broad peaks at 22 °C. The NMR spectral features of the $Ir-CH_3$ group are similar to those of **10a** and **10b** and to that in the structurally similar (Me trans to an empty site) Milstein's (PCP)Ir(Me)Cl.[10c,d] The ^1H NMR resonances arising from $N-CH_2-Ir$ in **16c** (δ 3.78 ppm, J_{HP} = 11 Hz, J_{CH} = 140 Hz) and $Ir-CH_3$ in **10c** (δ 2.37 ppm,

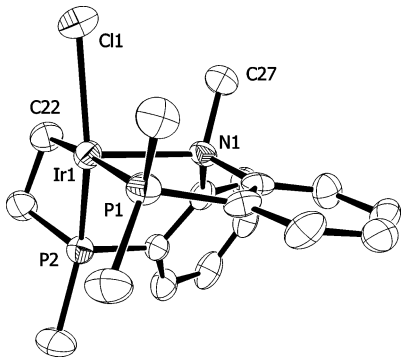

Figure 11. ORTEP drawing (50% probability ellipsoids) of **11a** showing selected atom labeling.[17] Omitted for clarity: H atoms, methyls of the ^{i}Pr groups. Selected distances (Å) and angles (deg) follow: Ir1−P1, 2.288(3); Ir1−P2, 2.214(3); Ir1−C22, 2.164(10); Ir1−N1, 2.340(7); Ir1−Cl1, 2.440(3). P1−Ir1−P2, 107.56(9); P1−Ir1−C22, 174.2(3); P2−Ir1−C22, 66.9(3); P1−Ir1−N1, 84.29(18); P2−Ir1−N1, 83.53(19); C22−Ir1−N1, 93.2(3); P1−Ir1−Cl1, 97.02(9); P2−Ir1−Cl1, 155.28(9); C22−Ir1−Cl1, 88.5(3); N1−Ir1−Cl1, 96.69(19).

Scheme 7

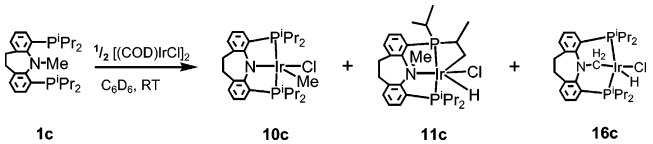

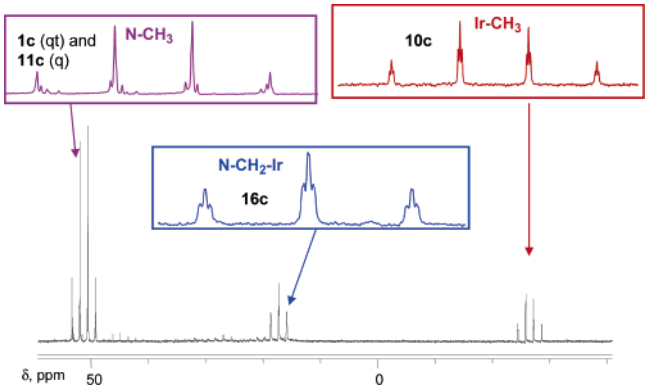

Figure 12. Undecoupled ^{13}C NMR spectra of the reactions of **1a-*^{13}C*** (top) and **1c-*^{13}C*** (bottom) with [(COD)IrCl]$_2$.

Scheme 8

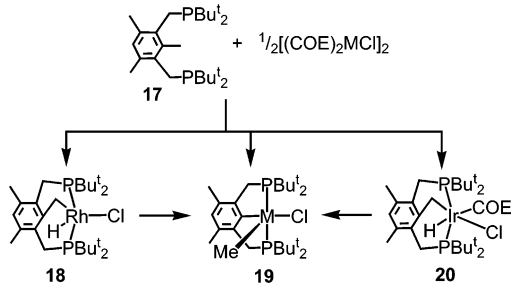

J_{HP} = 6 Hz, J_{CH} = 138 Hz) were identified in the reaction mixture in part by comparison between the spectra of the ^{13}C-labeled and unlabeled samples (J_{C-H} is known from the ^{13}C NMR spectra). The hydride signal of **16c** resonates at δ −25.7 ppm (t, J_{HP} = 19 Hz) in the ^{1}H NMR spectrum. Identification of ^{31}P NMR resonances of **16c** and **11c** is also possible by the magnitude of the J_{C-P} coupling constants that are known from the ^{13}C NMR spectra. Comparison with the spectra resulting from the reactions of **1a-*^{13}C*** and **1c-*^{13}C*** with [(COD)IrCl]$_2$ is also helpful. We have not observed any ^{13}C NMR resonances attributable to the product of activation of the C−H bonds of N−CH$_3$ (analogue of **16c**) in the reaction of **1a-*^{13}C*** (or **1a** and **1b**) with [(COD)IrCl]$_2$.

Structural Features of 9c and 16c in Solution. The ^{13}C-labeling experiments clearly demonstrate that an N−CH$_2$−M (M = Rh, Ir) unit is present in **9c** and **16c**. Presumably, this is formed from the N−CH$_3$ group in the ligand via C−H oxidative addition to the metal center. Each of **9c** and **16c** bears a hydride on the metal center. While it appears that **9c** and **16c** are only different by the metal center (Rh vs Ir), they clearly possess *different* symmetry (C_1 vs C_s) and are thus are not isostructural. Milstein et al. have observed related C−H activation of the central C−CH$_3$ group in the PC(CH$_3$)P pincer **17** with both Rh and Ir (Scheme 8).[10c,d] In Milstein's case, however, both metals gave rise to compounds of the same C_s symmetry (**18** and the Ir analogue **20** as an adduct with cyclooctene). In part, this can be ascribed to the immense steric bulk of the PBu$^t_2$ groups in the Milstein's ligand that disfavors cis-phosphine disposition. A later theoretical study of the Milstein system by Hall et al. found that the observed C_s-diastereomer for the C−H activation products **18** and **20** is indeed thermodynamically preferred for the model system **21** (Scheme 9).[23] However, Hall's study also revealed that (at least for the sterically modest model

Scheme 9

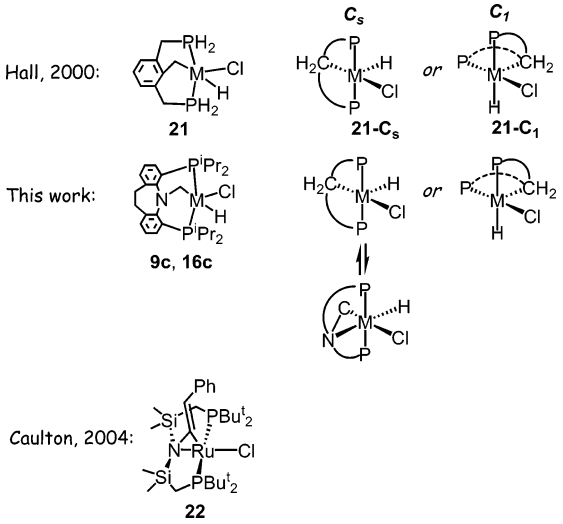

PCP ligand in **21**) the C_1 diastereomer is only <3 kcal/mol higher in energy for either Rh and Ir. We propose that **9c** possesses a structure qualitatively analogous to this C_1 isomer computationally discovered by Hall (Scheme 9).[23] This structure accounts for the observed NMR data. The hydride is clearly trans to one of the phosphine arms given the mammoth J_{HP} = 160 Hz. The phosphines are thus cis(oid), probably with an angle close to that in **11a** (Figure 11). The observed broadness of the peaks typical for the THPNP complexes would mask possible coupling of smaller magnitude. The CH$_2$ group must be cis to both phosphines, and a concerted C−H oxidative addition process should place CH$_2$ and H cis to each other in the product. We propose a five-coordinate structure with a CH$_2$ (strongest trans-influence ligand) trans to the empty site and Cl trans to one of the phosphines.[24] The two J_{P-Rh} coupling constants are consistent with this picture. Selective decoupling ^{1}H{^{31}P} experiments showed that the hydride in **9c** is trans to the phosphine that resonates at δ −5.1 ppm. This phosphorus nucleus displays a much lower J_{P-Rh} (92 Hz) than the other P (δ 55.1 ppm, J_{P-Rh} = 190 Hz). A longer Rh−P bond and therefore a lower J_{P-Rh} is expected for P trans to a stronger trans-influence ligand such as hydride. For instance, in (MeC(CH$_2$PPh$_2$)$_3$)Rh(H)$_2$Cl, the phosphines trans to H display J_{P-Rh} = 78 Hz, while the one trans to Cl displays J_{P-Rh} = 138 Hz.[25] Interestingly, the average J_{P-Rh} = 141 Hz in **9c** is close to the J_{P-Rh} = 140 Hz observed in the C_s-symmetric **18**.

The solution NMR data for **16c** are consistent with the proposed C_s structure. It is not clear why the two metals prefer different structures. Since we only observe **9c** and **16c** as components of mixtures, we cannot exclude that small amounts of the other isomer are also present. There is not sufficient evidence to determine

(23) Cao, Z.; Hall, M. B. *Organometallics* **2000**, *19*, 3338.
(24) The pertinent analysis of the structural preferences of five-coordinate d^6 complexes can be found elsewhere. (a) Lam, W. H.; Shimada, S.; Batsanov, A. S.; Lin, Z.; Marder, T. B.; Cowan, J. A.; Howard, J. A. K.; Mason, S. A.; McIntyre, G. J. *Organometallics* **2003**, *22*, 4557. (b) Rachidi, I. E.-I.; Eisenstein, O.; Jean, Y. *New J. Chem.* **1990**, *14*, 671. (c) Riehl, J.-F.; Jean, Y.; Eisenstein, O.; Pelissier, M. *Organometallics* **1992**, *11*, 729. (d) Olivan, M.; Eisenstein, O.; Caulton, K. G. *Organometallics* **1997**, *16*, 2227.
(25) Bianchini, C.; Meli, A.; Peruzzini, M.; Vizza, F.; Frediani, P.; Ramirez, J. A. *Organometallics* **1990**, *9*, 226.

whether N is bound to Ir in **16c** or to Rh in **9c**. A recent example from Caulton et al. shows that N and C simultaneously can be bound to the transition metal (Ru) in a closely related environment (**22**, Scheme 9).[26] Binding of N to Rh in a C_1-symmetric structure (Scheme 9) proposed for **9c** seems spatially improbable. On the other hand, in a C_s-symmetric structure proposed for **16c**, N is located cis to the empty site and may ostensibly coordinate to Ir. Ir generally makes stronger bonds to ligands than Rh and thus has a higher preference for saturation (cf. cyclooctene coordination to Ir in **20**). Conceivably, the greater benefit of the N−M bond for M = Ir may contribute to the observed structural preference (**9c-*C*$_1$** vs **16c-*C*$_s$**).

Isomerization of Cyclooctadiene and Deuterium Labeling Experiments. In all of the reactions of ligands **1a**−**c** with $[(COD)MCl]_2$ (M = Rh, Ir) we have observed isomerization of 1,5-COD to 1,3-COD with intermediate formation of 1,4-COD. This was rather peculiar because not in all of these cases were metal hydride complexes present. The most common mechanism of olefin isomerization is via insertion/elimination into a metal−hydride bond.[27] Hydrides **11a**−**c** are saturated and without any obviously labile ligands and thus unsuitable for isomerization catalysis. In fact, an isolated sample of **11a** did not isomerize 1,5-COD in a separate experiment. It appeared plausible that in some cases unobserved metal hydrides present in small concentration were responsible for the isomerization of COD. Since the coordination of N to the metal center in **9c** and **16c** either is not present or is labile (vide supra), then **9c**, **16c**, or analogous compounds would be perfect candidates for the isomerization catalyst. To test this hypothesis, we prepared the CD_3-labeled ligands **1a-*d*$_3$** and **1c-*d*$_3$** and allowed each to react with either $[(COD)RhCl]_2$ or $[(COD)IrCl]_2$ in C_6H_6. Isomerization of 1,5-COD into 1,3-COD occurs in all cases. ^{2}H NMR analysis of the volatile material revealed incorporation of D into 1,3-COD (^{2}H NMR: δ 5.84, 5.52, 2.02, 1.33 ppm) in the reactions of **1c-*d*$_3$**, but not in those of **1a-*d*$_3$**. The isomerization of 1,5-COD into 1,3-COD in general is much faster for the reactions of **1c** compared to **1a** or **1b**. These results are consistent with the observation of distinct **9c** and **16c**, but not their analogues with "untied" PNP ligands. It seems reasonable to propose that the activation of the C−H bonds of the N−Me group does occur with **1a** and **1b**, but only to an undetectably small extent (unless isomerization to the N−C activation product is much faster than isomerization of COD). Examples of selective activation of the α-CH bonds in amines have been reported.

PCP vs PNP. The reactivity displayed by the PN(Me)P pincer ligands with Rh^I and Ir^I is generally that of oxidative addition of the N−C and/or surrounding C−H bonds to the metal center. This partly parallels the topologically similar PCP chemistry investigated by Milstein et al.[10] The topological similarity is additionally reinforced by the fact that in our study the product of the C−H activation of the $N-CH_3$ group is much less stable for Rh (**9c**, $t_{1/2}(298) < 30$ min) than for Ir (**16c**, stable at ambient temperature) with respect to the product of the N−C OA. PCP analogues behave similarly: the Ir compound **20** is stable at ambient temperature while the Rh compound **18** slowly (hours) isomerizes to the C−C OA product **19**.[10c−e] In the case of Ir, the marked difference of our PNP reactivity from the PCP analogues is the isolation of distinct products (**11a**−**c**) of oxidative addition of the pendant C−H bonds of the ^{i}Pr groups.

The differences in the structural preferences of the PNP-derived products (vide supra) compared with the PCP chemistry may seem to stem from the change from C to N in the central pincer atom. However, one must also take into account that in reactions of the "untied" ligands **1a** and **1b** no products of the C−H activation of the $N-CH_3$ were observed at all. With that in mind, we are forced to conclude that the balance between C−H and N−C activation (or that of C−C, and likely of C−X in general) in both the kinetic and the thermodynamic sense depends not only on the nature of the donor atoms in the pincer ligand but also on the rigidity and connectivity of the pincer framework.

Conclusion. Introduction of a $-CH_2CH_2-$ unit as a linker of the two aromatic rings in the diarylamido-based PNP ligands (cf., the "tied" ligand **1c**) translates into detectable differences in reactivity of the various PNP ligands with monovalent Rh and Ir. The "tied" ligand **1c** is also effectively bulkier than its "untied" analogues **1a** and **1b**.

Monovalent Rh and Ir undergo oxidative addition of N−C and C−H bonds in the context of the diarylamido-based PNP ligands. The positioning of the transition metal center in the vicinity of the pendant N−C and C−H bonds via coordination to the two phosphine donors undoubtedly facilitates these processes. However, the differences between the reactivity of Rh and Ir observed here may reflect the general trend: compared with Rh(I) in a similar environment, Ir(I) displays a pronounced preference for C−H oxidative addition over C−heteroatom oxidative addition.

The selectivity for N−C activation is enhanced by changing the reaction phase from solution to the solid state, as exemplified by the regiospecific solid-state thermolysis of **7b**. This aspect of the reported reactivity is unexpected, and the reasons for such selectivity are not well understood. A drastic and desirable selectivity change in an organometallic reaction upon the change of the reaction phase to the solid state is an event with an underdeveloped potential[21] and merits a separate in-depth study.

Experimental Section

General Considerations. Unless specified otherwise, all manipulations were performed under an argon atmosphere using standard Schlenk line or glovebox techniques. Toluene, pentane, Et_2O, C_6D_6, C_6H_6, THF, and iso-octane were dried over NaK/Ph_2CO/18-crown-6, distilled or vacuum transferred, and stored over molecular sieves in an Ar-filled glovebox. Fluorobenzene was dried with and then distilled from CaH_2. Compounds $(COD)PdCl_2$,[28] $[(COD)RhCl]_2$,[29] $[(COD)IrCl]_2$,[30] **1a**,[2a] **1b**,[1a,8d] **6a**,[8e] **7a**,[2a] **8a**,[2a] and **10a**[2a] were prepared according to published procedures. All other chemicals were used as received from commercial vendors. NMR spectra were recorded on a Varian iNova 400 (^{1}H NMR, 399.755 MHz; ^{13}C NMR, 100.518 MHz; ^{31}P NMR, 161.822 MHz; ^{2}H, 61.365 MHz) spectrometer. The ^{1}H NMR spectrum of **9c** was also re-

(26) Walstrom, A. M.; Watson, L. A.; Pink, M.; Caulton, K. G. *Organometallics* **2004**, *23*, 4814.

(27) Crabtree, R. H. *The Organometallic Chemistry of the Transition Metals*, 3rd ed.; Wiley-Interscience: New York, 2001; p 226.

corded on a Varian iNova 500 spectrometer. Chemical shifts are reported in δ (ppm). For ^{1}H and ^{13}C NMR spectra, the residual solvent peak was used as an internal reference. ^{31}P NMR spectra were referenced externally using 85% H_3PO_4 at δ 0 ppm. ^{19}F NMR spectra were referenced externally to 1.0 M CF_3CO_2H in $CDCl_3$ (Wilmad) at δ −78.5 ppm. Elemental analyses were performed by CALI Labs, Inc. (Parsippany, NJ).

X-ray Structure Determination. Single crystals of **1b** suitable for X-ray diffraction measurements were obtained from a saturated solution in hexamethyldisiloxane upon standing. Single crystals of **1d** were obtained by crystallization from a saturated ethanol solution at −35 °C. Single crystals of **6c** were obtained by cooling an ether solution to −35 °C overnight. Single crystals of **11a** were obtained by recrystallization from ether/PhF at −35 °C. Crystals were mounted in glass capillaries. Data collection was carried out at room temperature (low-temperature apparatus was not available) on a CAD-4 Turbo diffractometer equipped with Mo Kα radiation (**6c** and **11a**) and a CAD-4U diffractometer equipped with Cu Kα radiation (**1b** and **1d**).[31] The structures were solved by direct methods (SIR92).[32] Full-matrix least-squares refinement was carried out using the Oxford University *Crystals for Windows* system.[33] All ordered non-hydrogen atoms were refined using anisotropic displacement parameters; hydrogen atoms were fixed at calculated geometric positions and updated after each least-squares cycle.

^{Me}PN(^{13}CH$_3$)P (1a-^{13}*C*) and ^{Me}PN(CD$_3$)P (1a-*d*$_3$) were prepared according to the previously published procedure for the synthesis of **1a** utilizing $^{13}CH_3I$ and CD_3I, respectively.[2a] Selected NMR data follow: For **1a-^{13}*C***, ^{1}H NMR (C_6D_6): δ 3.50 (d, 3H, J = 136 Hz, N−C*H*$_3$). ^{31}P{^{1}H} NMR (C_6D_6): δ −6.8 (d, J_{P-C} = 9 Hz); For **1a-*d*$_3$**, ^{2}H NMR (C_6D_6): δ 3.45 (s).

THPN(Me)P (1c). *n*-BuLi (2.00 mL of a 2.5 M solution in hexanes, 4.96 mmol) was slowly added to **1d** (1.5 g, 2.48 mmol) dissolved in 20 mL of ether. The mixture was stirred for 1 h. Then 1 mL of methanol was added to the mixture, and it was stirred for 30 min. All volatiles were removed in vacuo, and the residue was dissolved in pentane and passed through a pad of silica gel. The resulting solution was concentrated to ca. 5 mL and cooled to −35 °C. The precipitate was collected the next day and dried under vacuum. Yield: 894 mg (82%). Anal. Calcd for $C_{27}H_{41}NP_2$: C, 73.44; H, 9.36. Found: C, 73.28; H, 9.49. ^{1}H NMR (C_6D_6): δ 7.30 (d, 2H, $^3J_{HH}$ = 7 Hz, Ar−*H*), 6.98 (t, 2H, $^3J_{HH}$ = 7 Hz, Ar−*H*), 6.90 (d, 2H, $^3J_{HH}$ = 7 Hz, Ar−*H*), 3.46 (s, 3H, N−*Me*), 3.05 (dd, 2H, J = 8 Hz, J = 14 Hz, C*H*$_a$H$_b$C*H*$_a$H$_b$), 2.53 (dd, 2H, J = 8 Hz, J = 14 Hz, CH$_a$*H*$_b$CH$_a$*H*$_b$), 1.99 (m, 4H, C*H*Me$_2$), 1.27 (app. quartet (dvt), 12H, CH*Me*$_2$), 1.16 (app. quartet (dvt), 6H, CH*Me*$_2$), 1.06 (app. quartet (dvt), 6H, CH*Me*$_2$). ^{31}P{^{1}H} NMR (C_6D_6): δ −8.8 (s). ^{13}C NMR (C_6D_6): δ 155.2 (t, J = 11 Hz), 139.7 (s), 138.8 (t, J = 11 Hz), 131.8 (s), 131.0 (s), 125.0 (s), 51.3 (t, J = 11 Hz, N-*Me*), 33.8 (s, −*C*H$_2$*C*H$_2$−), 27.3 (t, J = 8 Hz, *C*HMe$_2$), 26.1 (t, J = 8 Hz, *C*HMe$_2$), 21.7 (app. quartet (dvt), CH*Me*$_2$), 20.5 (app. quartet (dvt), CH*Me*$_2$).

^{TBr}PN(^{13}CH$_3$)P (1d-^{13}*C*). NaH (0.17 g, 7 mmol) and **4** (3.25 g, 6.36 mmol) were mixed in ca. 20 mL of THF. The mixture was stirred for 2 h, and $^{13}CH_3I$ (438 μL, 7 mmol) was added. The resulting mixture was stirred for another 12 h. All volatiles were removed under vacuum. The residue was extracted with ether in two portions and passed through a Celite pad. *n*-BuLi (5.78 mL, 12.5 M) was added to the resulting ether solution at −35 °C. The mixture was allowed to warm to room temperature and stirred for 2 h. Chlorodiisopropylphosphine (2.0 mL, 12.5 mmol) was added to the mixture and stirred for 12 h. Then ∼1 mL of MeOH was added, and this was stirred for 0.5 h. The volatiles were removed in vacuo, and the residue was dissolved in pentane and passed through a pad of silica gel. The resulting solution was concentrated and kept in the refrigerator at −35 °C. The next day the white precipitate of **1d-^{13}C** was collected. Yield: 2.0 g (53%). Selected NMR data follow: ^{1}H NMR (C_6D_6): δ 3.24 (d, J = 136 Hz, 3H, N−^{13}C*H*$_3$). ^{31}P{^{1}H} NMR (C_6D_6): δ −7.7 (d, J = 10 Hz).

THPN(^{13}CH$_3$)P (1c-^{13}*C*). *n*-BuLi (967 μL, 2.2 mmol) was added to an ether solution of **1d-^{13}*C*** (638 mg, 1.06 mmol) at −35 °C. After stirring at ambient temperature for 2 h, 0.2 mL of MeOH was added, and this was stirred for 0.5 h. All volatiles were removed under vacuum, and the residue was dissolved in pentane and passed through silica gel. The pentane solution was evaporated in vacuo to give an oily residue. This residue was triturated with 10 mL of MeOH to afford **1c-^{13}*C*** as a white solid. Yield: 280 mg (60%). Selected NMR data follow: ^{1}H NMR (C_6D_6): δ 3.46 (d, J = 136 Hz, 3H, N−^{13}C*H*$_3$). ^{31}P{^{1}H} NMR (C_6D_6): δ −8.9 (d, J = 10 Hz).

^{TBr}PN(Me)P (1d). *n*-BuLi (3.76 mL of 2.5 M solution in hexanes, 9.40 mmol) was slowly added to a solution of **5** (2.5 g, 4.7 mmol) in 30 mL of Et_2O at ambient temperature. The mixture was stirred for 1 h. Then chlorodiisopropylphosphine (1.50 mL, 9.40 mmol) was added to the mixture, and it was stirred for 12 h. The volatiles were removed in vacuo, and the residue was dissolved in pentane and filtered. The filtrate was treated with silica gel and stirred for 30 min, and then the solids were filtered off. The resulting solution was evaporated in vacuo to afford a pale yellowish oil. This oil was triturated with methanol to produce a white solid. The solid was collected by filtration. Yield: 1.7 g (60%). ^{1}H NMR (C_6D_6): δ 7.54 (d, 2H, J = 2 Hz, Ar−*H*), 7.00 (d, 2H, J = 2 Hz, Ar−*H*), 3.25 (s, 3H, N−*Me*), 2.68 (dd, 2H, C*H*$_a$H$_b$C*H*$_a$H$_b$, J = 10 Hz, J = 16 Hz), 2.16 (dd, 2H, CH$_a$*H*$_b$CH$_a$*H*$_b$, J = 10 Hz, J = 16 Hz), 1.80 (m, 4H, −C*H*Me$_2$), 1.13 (app. quartet (dvt), 12H, CH*Me*$_2$), 1.03 (app. quartet (dvt), 6H, CH*Me*$_2$), 0.92 (app. quartet (dvt), 6H, CH*Me*$_2$). ^{31}P{^{1}H} NMR (C_6D_6): δ −7.7 (s). ^{13}C NMR (C_6D_6): δ 153.6 (t, J = 11 Hz), 142.1 (t, J = 13 Hz), 141.7 (s), 134.3 (s), 133.7 (s), 119.0 (s), 50.9 (t, J = 10 Hz, N−*Me*), 32.8 (s, *C*H$_2$*C*H$_2$), 27.3 (t, J = 7 Hz, *C*HMe$_2$), 26.0 (t, J = 8 Hz, *C*HMe$_2$), 21.5 (app. quartet (dvt), CH*Me*$_2$), 20.2 (app. quartet (dvt), CH*Me*$_2$). The selected ^{1}H NMR data collected while decoupling the ^{31}P signal at −7.7 ppm follow: 7.53 (d, 2H, $^4J_{HH}$ = 2 Hz, Ar−*H*), 7.01 (d, 2H, $^4J_{HH}$ = 2 Hz, Ar−*H*), 1.13 (d, 12H, J = 7 Hz, CH*Me*$_2$), 1.03 (d, 6H, J = 7 Hz, CH*Me*$_2$), 0.92 (d, 6H, J = 7 Hz, CH*Me*$_2$).

^{TBr}(PN(CD$_3$)P) (1d-*d*$_3$) and **THPN(CD$_3$)P (1c-*d*$_3$)** were prepared similarly to **1c-*^{13}C*** and **1d-*^{13}C*** using CD_3I. ^{2}H NMR data follow: **1d-*d*$_3$**: ^{2}H NMR (C_6H_6): δ 3.17 (s). **1c-*d*$_3$**: ^{2}H NMR (C_6H_6): δ 3.37 (s).

(THPNP)PdCl (6c). (COD)$PdCl_2$ (56 mg, 0.196 mmol) was added to the solution of **1c** (79 mg, 0.180 mmol) in 10 mL of toluene with stirring, and the color of the solution rapidly changed to dark red. The mixture was heated at 90 °C for 30 min while being stirred, and then the resulting mixture was passed through Celite. The volatiles were removed from the filtrate in vacuo to produce 54 mg (80%) of a purple solid. ^{1}H NMR (C_6D_6): δ 6.75 (m, 4H, Ar−*H*), 6.41 (d, 2H, J = 7 Hz, Ar−*H*), 2.86 (s, 4H, −C*H*$_2$C*H*$_2$−), 2.30 (m, 4H, C*H*Me$_2$), 1.42 (app. quartet (dvt), 12H, CH*Me*$_2$), 1.22 (m, 12H, CH*Me*$_2$). ^{31}P{^{1}H}NMR (C_6D_6): δ 49.4 (s). ^{13}C NMR (C_6D_6): δ 162.8 (t, J = 10 Hz), 134.6 (t, J = 6 Hz), 133.8 (s), 130.6 (s), 121.1 (t, J = 18 Hz), 115.8 (t, J = 4 Hz), 40.6 (s, −*C*H$_2$*C*H$_2$−), 25.0 (br s, *C*HMe$_2$), 18.6 (s, CH*Me*$_2$), 17.7 (s, CH*Me*$_2$).

Reaction of 1a/1a-^{13}*C* with [Rh(COD)Cl]$_2$. To two J. Young NMR tubes was added **1a** and **1a-^{13}*C*** (25 mg, 0.056

(28) Drew, D.; Doyle, J. R. *Inorg. Synth.* **1990**, 28, 346.
(29) Giordano, G.; Crabtree, R. H. *Inorg. Synth.* **1979**, *19*, 218.
(30) Crabtree, R. H.; Morris, G. E. *J. Organomet. Chem.* **1977**, *135*, 395.
(31) Straver, L. H. *CAD4-EXPRESS*, Enraf-Nonius: Delft, The Netherlands, 1992.
(32) Altomare, A.; Cascarano, G.; Giacovazzo G.; Guagliardi A.; Burla M. C.; Polidori, G.; Camalli, M. *J. Appl. Crystallogr.* **1994**, *27*, 435.
(33) Betteridge, P. W.; Carruthers, J. R.; Cooper, R. I.; Prout, K.; Watkin, D. J. *J. Appl. Crystallogr.* **2003**, *36*, 1487.

mmol), respectively. $[Rh(COD)Cl]_2$ (14 mg, 0.056 mmol Rh) and C_6D_6 (0.5 mL) were added to each of these two tubes, and the mixtures were shaken well. The reaction was monitored by ^{31}P, ^{1}H, and ^{13}C NMR. **7a/7a-*13C*** was formed near-quantitatively in less than 10 min with a trace of **1a/1a-*13C*** observed. The conversion of **7a/7a-*13C*** to **8a/8a-*13C*** is very slow, and the reaction was not completed after 24 h. ^{1}H NMR data indicate that 1,5-COD released in the beginning was converted into 1,4-COD and eventually into 1,3-COD. The isomerization of 1,5-COD is not completed in 5 h. Selected NMR data for **7a/7a-*13C*** follow: ^{1}H NMR (C_6D_6): δ 3.72 (s, N-*Me*) for **7a**; 3.72 (d, J_{C-H} = 141 Hz, N−*Me*) for **7a-*13C***. $^{31}P\{^{1}H\}$ NMR (C_6D_6): δ 32.5 (d, J_{Rh-P} = 154 Hz). $^{13}C\{^{1}H\}$ NMR (C_6D_6): δ 62.7 (app q, J = 2, N-Me). ^{13}C NMR (C_6D_6): δ 62.7 (q, J_{C-H} = 140 Hz, N−*Me*). Selected NMR data for **8a/8a-*13C*** follow: ^{1}H NMR (C_6D_6): δ 2.33 (dt, J_{H-P} = 5, J_{H-Rh} = 3, Rh−*Me*) for **8a**; 2.33 (ddt, J_{H-P} = 5, J_{H-Rh} = 3, J_{C-H} = 141, Rh−*Me*) for **8a-*13C***. $^{31}P\{^{1}H\}$ NMR (C_6D_6): δ 36.2 (d, J_{Rh-P} = 109 Hz). $^{13}C\{^{1}H\}$ NMR (C_6D_6): δ 1.9 (dt, J_{C-Rh} = 29, J_{C-P} = 5, Rh−*Me*). ^{13}C NMR (C_6D_6): δ 1.9 (qdt, J_{C-Rh} = 29, J_{C-P} = 5, J_{C-H} = 141, Rh−*Me*).

Reaction of 1c/1c-^{13}*C* with [Rh(COD)Cl]$_2$. To two J. Young NMR tubes was added **1c** and **1c-^{13}*C*** (25 mg, 0.056 mmol), respectively. $[Rh(COD)Cl]_2$ (14 mg, 0.056 mmol Rh) and C_6D_6 (0.5 mL) were added to each tube, and the mixtures were vigorously shaken and were allowed to stand at ambient temperature while being periodically monitored by NMR. The reaction mixture became noticeably green in less than 2 h, and the final deep green color was attained in less than 4 h. After 30 min, **7c**, **8c**, and **9c** were observed in a 4:7:4 ratio. The NMR resonance of **9c** disappeared after 1 h. After 7 h **8c/8c-*13C*** was observed as the dominant product (>95%) (excluding a small amount of adventitious excess of **1c**). ^{1}H NMR analysis indicated that 1,5-COD released in this reaction was completely converted into 1,3-COD within 1 h. Selected NMR data for **7c** follow: ^{1}H NMR (C_6D_6): δ 4.12 (s, N−*Me*) for **7c**; 4.12 (d, J_{C-H} = 141 Hz, N−*Me*) for **7c-*13C***. $^{31}P\{^{1}H\}$ NMR (C_6D_6): δ 34.4 (d, J_{Rh-P} = 151 Hz). $^{13}C\{^{1}H\}$ NMR (C_6D_6): δ 60.8 (s, N−Me). ^{13}C NMR (C_6D_6): δ 60.8 (q, J_{C-H} = 140 Hz, N−*Me*). Selected NMR data for **8c-*13C*** follow: ^{1}H NMR (C_6D_6): δ 2.33 (ddt, J_{H-P} = 5, J_{H-Rh} = 3, J_{C-H} = 141, Rh−*Me*) for **8c-*13C***. ^{13}C NMR (C_6D_6): δ 3.75 (qdt, J_{C-Rh} = 29, J_{C-P} = 5, J_{C-H} = 141, Rh−*Me*). Selected NMR data for **9c/9c-*13C*** follow: ^{1}H NMR (C_6D_6): δ 2.53 (m, Rh−C*H*$_2$), −9.67 (br, d, J_{H-P} = 160 Hz, Rh−*H*). The observed 160 Hz coupling is to the ^{31}P NMR signal at δ −5.1 ppm as established by selective $^{1}H\{^{31}P\}$ decoupling experiments. The same 160 Hz J_{H-P} was observed on both the 400 MHz and the 500 MHz spectrometers. $^{31}P\{^{1}H\}$ NMR (C_6D_6): δ 55.1 (br, d, J_{P-Rh} = 190 Hz), −5.1 (br, d, J_{P-Rh} = 92 Hz). $^{13}C\{^{1}H\}$ NMR (C_6D_6): δ 41.7 (d, J_{Rh-C} = 20 Hz). ^{13}C NMR (C_6D_6): δ 41.7 (td, J_{Rh-C} = 20 Hz, J_{C-H} = 140 Hz).

(^{F}PN(Me)P)RhCl (7b). In a 50 mL Schlenk flask **1b** (160 mg, 0.355 mmol) was dissolved a mixture of 4 mL of Et_2O and 2 mL of PhF. $[(COD)RhCl]_2$ (84 mg, 0.171 mmol) was added to this flask, and the mixture was stirred for 5 min. The product was recrystallized by removing the volatiles under vacuum followed by dissolving the residue in 2 mL of PhF, layering with Et_2O, and placing in the −35 °C freezer overnight. Yield: 137 mg (68%). ^{1}H NMR (C_6D_6): δ 7.07 (app. dq, 2H, 8 Hz, 3 Hz, Ar−*H*), 6.64 (dd, 2H, 10 Hz, 5 Hz, Ar−*H*), 6.57 (app. td, 2H, 8 Hz, 3 Hz, C*H*), 3.54 (s, 3H, N−C*H*$_3$), 2.23 (m, 4H, C*H*Me$_2$), 1.55 (app. quartet (dvt), 6H, J_{HP} = 8 Hz, C*H*$_3$), 1.40 (app. quartet (dvt), 6H, J_{HP} = 8 Hz, C*H*$_3$), 1.14 (app. quartet (two dvt), 12H, J_{HP} = 7 Hz, C*H*$_3$). $^{13}C\{^{1}H\}$ NMR (C_6D_6): δ 161.2 (d, 251 Hz, *C*−F), 156.8 (td, 9 Hz, 2 Hz, *C*−N), 141.1 (m), 123.0 (m), 119.1 (d, 21 Hz), 115.3 (d, 23 Hz), 63.2 (s, N*C*H$_3$), 27.8 (t, 11 Hz, *C*H(CH$_3$)$_2$), 27.4 (t, 8 Hz, *C*H(CH$_3$)$_2$), 20.5 (t, 3 Hz, CH(*C*H$_3$)$_2$), 19.9 (br s, CH(*C*H$_3$)$_2$), 19.7 (t, 3 Hz, CH(*C*H$_3$)$_2$), 19.5 (t, 3 Hz, CH(*C*H$_3$)$_2$). $^{31}P\{^{1}H\}$ NMR (C_6D_6): δ 32.8 (d, J_{P-Rh} = 154 Hz). ^{19}F NMR (C_6D_6): δ −118.6 (m).

Thermolysis of (^{F}PN(Me)P)RhCl (7b) in Solution. A sample of solid, freshly crystallized **7b** (25 mg, 42 μmol) was placed in a J. Young NMR tube and dissolved in 0.6 mL of C_6D_6 in a glovebox. The tube was placed in a 70 °C oil bath for 2 h. NMR analysis revealed the complete consumption of **7b** and the formation of a mixture containing ca. 70% of **8b** and a number of unidentified compounds.

(^{F}PNP)Rh(Me)Cl (8b) by Solid-State Thermolysis of 7b. A sample of solid, freshly crystallized **7b** (21 mg, 36 μmol) was placed in a small screw-capped tube in a glovebox. This tube was placed in a 70 °C oil bath for 3 h. The tube was taken back into a glovebox, and the entire solid sample was dissolved in C_6D_6. NMR analysis revealed the presence of *only* **8b**. ^{1}H NMR (C_6D_6): δ 7.44 (m, 2H, Ar−*H*), 6.81 (m, 2H, Ar−*H*), 6.63 (m, 2H, Ar−*H*), 2.46 (m, 2H, C*H*Me$_2$), 2.22 (dt, J_{H-P} = 5 Hz, J_{H-Rh} = 3 Hz, 3H, Rh−*Me*), 2.15 (m, 2H, C*H*Me$_2$), 1.38 (app. quartet (dvt), 6H, 8 Hz, CH*Me*$_2$), 1.05 (app. quartet (dvt), 6H, 8 Hz, CH*Me*$_2$), 1.03 (app. quartet (dvt), 6H, 8 Hz, CH*Me*$_2$), 0.85 (app. quartet (dvt), 6H, 8 Hz, CH*Me*$_2$). $^{1}H\{^{31}P\}$ NMR (C_6D_6): δ 7.44 (dd, 2 H, 10 Hz, 5 Hz, Ar−*H*), 6.81 (dd, 2H, 8 Hz, 3 Hz, Ar−*H*), 6.63 (ddd, 2H, 10 Hz, 8 Hz, 3 Hz, Ar−*H*), 2.46 (septet, 2H, 7 Hz, C*H*Me$_2$), 2.22 (d, J_{H-Rh} = 3 Hz, 3H, Rh−*Me*), 2.15 (septet, 2H, 7 Hz, C*H*Me$_2$), 1.38 (d, 6H, 7 Hz, CH*Me*$_2$), 1.05 (d, 6H, 7 Hz, CH*Me*$_2$), 1.03 (d, 6H, 7 Hz, CH*Me*$_2$), 0.85 (d, 6H, 7 Hz, CH*Me*$_2$). $^{13}C\{^{1}H\}$ NMR (C_6D_6): δ 159.8 (vt, J_{CP} = 10 Hz, aryl N−*C*), 154.7 (dvt, J_{C-F} = 238 Hz, J_{C-P} = 3 Hz), 121.9 (vtd, J_{C-F} = 5 Hz, J_{C-P} = 16 Hz), 118.2 (d, J_{C-F} = 21 Hz, J_{C-P} = 16 Hz), 117.9 (br s), 117.8 (d, 22 Hz), 26.9 (vt, J_{C-P} = 11 Hz, *C*HMe$_2$), 24.1 (vt, J_{C-P} = 11 Hz, *C*HMe$_2$), 19.4 (s, CH*Me*$_2$), 19.1 (s, CH*Me*$_2$), 18.0 (s, CH*Me*$_2$), 17.7 (s, CH*Me*$_2$), 2.3 (dt, J_{C-Rh} = 29 Hz, J_{CP} = 5 Hz, Rh−*C*H$_3$). $^{31}P\{^{1}H\}$ NMR (C_6D_6): δ 36.5 (d, J_{P-Rh} = 110 Hz). ^{19}F NMR (C_6D_6): δ −130.6 (m).

(THPNP)Rh(Me)Cl (8c), Preparative Isolation. 1c (120 mg, 0.27 mmol), $[(COD)RhCl]_2$ (66 mg, 0.27 mmol Rh), and 3 mL of toluene were placed in a Teflon-lined screw-capped tube. It was placed into a 60 °C oil bath for 3 h. The solution became deep green during this time. The tube was taken into a glovebox, and the contents were diluted with 10 mL of pentane and filtered to remove a small amount of insolubles. The filtrate was evaporated in vacuo to dryness, and the residue was recrystallized from cold pentane. Yield: 77 mg (50%). ^{1}H NMR (C_6D_6): δ 6.89 (br, 2 H, Ar−*H*), 6.77 (d, 2 H, $^{3}J_{HH}$ = 7 Hz, Ar−*H*), 6.49 (t, 2 H, $^{3}J_{HH}$ = 7 Hz, Ar−*H*), 2.90 (s, 4H, −CH$_2$CH$_2$−), 2.62 (br, 2H, C*H*Me$_2$), 2.33 (dt, J_{H-P} = 5 Hz, J_{H-Rh} = 3 Hz, 3H, Rh−*Me*), another C*H*Me$_2$ overlaps with the Rh−Me signal, 1.50 (br, 6H, CH*Me*$_2$), 1.14 (m, 12H, CHMe$_2$), 0.99 (d, 6H, J = 5 Hz). $^{31}P\{^{1}H\}$ NMR (C_6D_6, 25 °C): δ 42.6 (br), 36.7 (br). $^{31}P\{^{1}H\}$ NMR (C_6D_6, 50 °C): δ 39.7 (br). ^{13}C NMR (C_6D_6): δ 162.1 (br, s), 136.0 (br), 132.9 (s), 130.8 (s), 122.2 (br, s), 115.5 (t, J = 3 Hz), 40.9 (s, *C*H$_2$*C*H$_2$), 26.9 (t, J = 11 Hz, *C*HMe$_2$), 24.4 (br, *C*HMe$_2$), 19.6 (br, CH*Me*$_2$), 18.8 (s, CH*Me*$_2$), 17.8 (s, CH*Me*$_2$), 3.75 (dt, J_{Rh-C} = 29 Hz, J_{P-C} = 5 Hz). Anal. Calcd for $C_{27}H_{41}NP_2ClRh$: C, 55.92; H, 7.13. Found: C, 55.81; H, 7.25.

Thermolysis of 1a with [(COD)IrCl]$_2$. We have previously reported on the thermolysis of **1a** with $[(COD)IrCl]_2$ in C_6D_6 and PhF solvents. In both solvents a mixture of **10a** with the two isomers of **11a** was observed. At the time of the previous report, the nature of **11a** was not known. We have now fully characterized the major isomer of **11a** (vide infra). The selected NMR data for the minor isomer of **11a** were reported previously.

Isolation of Major Isomer of 11a. 1a (100 mg, 0.23 mmol), $[(COD)IrCl]_2$ (77.6 mg, 0.23 mmol Ir), and 10 mL of toluene were placed in a Teflon-lined screw-capped tube. It was placed into a 60 °C oil bath for 6 h. The solution became deep green during this time. The tube was taken into a glovebox, and the contents were diluted with 10 mL of toluene and filtered to remove a small amount of insolubles. The filtrate was evaporated to dryness in vacuo, and the residue was redissolved in ether. Cooling of the ether solution to −35 °C for 24 h resulted

in deposition of colorless crystalline material. It was filtered off, washed with cold pentane, and dried in vacuo. Yield: 50 mg (28%). The material contains <5% of the minor isomer of **11a**. Data for the major isomer of **11a** follow. ^{1}H NMR (C_6D_6): δ 7.27 (dd, 1H, J = 4 Hz, J = 8 Hz, Ar−*H*), 7.33 (dd, 1H, J = 4 Hz, J = 8 Hz, Ar−*H*), 7.25 (br, dd, 1H, J = 2 Hz, J = 6 Hz, Ar−*H*), 7.04 (d, 1H, J = 8 Hz, Ar−*H*), 6.95 (d, 1H, J = 8 Hz, Ar−*H*), 6.80 (d, 1H, J = 8 Hz, Ar−H), 3.81 (s, 3H, N−*Me*), 3.34 (m, 1H, C*H*Me$_2$), 3.21 (m, 1H, Ir−C*H*aH$_b$), 2.80 (m, 1H, C*H*Me$_2$), 2.04 (s, 3H, Ar−*Me*), 2.02 (s, 3H, Ar−*Me*), 1.96 (m, 1H, C*H*Me$_2$), 1.86 (m, 1H, C*H*Me$_2$), 1.65 (dd, 3H, J = 8 Hz, J = 16 Hz, CH*Me*$_2$), 1.51 (dd, 3H, J = 7 Hz, J = 14 Hz, CH*Me*$_2$), 1.15 (m, 6H, CH*Me*$_2$), 0.94 (dd, 3H, J = 7 Hz, J = 16 Hz, CH*Me*$_2$), 0.79 (dd, 3H, J = 7 Hz, J = 16 Hz, CH*Me*$_2$), 0.68 (dd, 3H, J = 7 Hz, J = 17 Hz, CH*Me*$_2$), 0.54 (m, 1H, Ir−CH$_a$*H*$_b$), −21.22 (1H, dd, J = 9 Hz, J = 16 Hz, Ir−*H*). ^{31}P{^{1}H} NMR (C_6D_6): δ 32.7 (s), −32.4 (s). ^{13}C NMR (C_6D_6): δ 160.6 (d, J = 18 Hz), 159.4 (d, J = 10 Hz), 138.9 (s), 138.7 (s), 136.0 (d, J = 4 Hz), 135.8 (d, J = 6 Hz), 133.2 (s), 132.7 (s), 131.8 (s), 131.5 (s), 125.3 (d, J = 8 Hz), 124.2 (d, J = 8 Hz), 53.6 (s, N−*Me*), 45.0 (d, J = 39 Hz), 30.0 (d, J = 23 Hz), 26.8 (d, J = 18 Hz), 24.6 (dd, J = 7 Hz, J = 9 Hz), 23.6 (J = 7 Hz), 21.6 (d, J = 16 Hz), 21.4 (s), 20.44 (s), 20.38 (s), 20.2 (s), 20.0 (d, J = 6 Hz), 19.3 (s), 18.1 (s), 2.60 (Ir−*C*H$_2$, J = 32 Hz, J = 79 Hz). Selected data for the minor isomer of **11a** follow. ^{1}H NMR (C_6D_6): δ 3.72 (s, N−*Me*), −20.92 (dd, J = 9 Hz, J = 16 Hz, Ir−*H*). ^{31}P{^{1}H} NMR (C_6D_6): δ 31.9 (s), −40.3 (s). Anal. (mixture of isomers of **11a**) Calcd for $C_{27}H_{43}ClIrNP_2$: C, 48.31; H, 6.46. Found: C, 48.43; H, 6.49.

Thermolysis of 1b with [(COD)IrCl]$_2$. 1b (22.5 mg, 50 mmol) and [(COD)IrCl]$_2$ (16.8 mg, 50 mmol Ir) were mixed in 0.6 mL of $PhCF_3$ in a J. Young NMR tube. After vigorously shaking the mixture at ambient temperature, a copious amount of yellow precipitate formed (presumably **12b**). This NMR tube was heated at 80 °C (oil bath) for 1 h. The solution became green during this time, and a small amount of white precipitate was visible. A 0.2 mL amount of CH_2Cl_2 was added to dissolve this precipitate. NMR analysis (^{19}F and ^{31}P) revealed the presence of **10b** and two isomers of **11b** in a 42:52:6 ratio in addition to traces of **1b** and a few other unidentified compounds totaling ca. 5% of the mixture. Selected NMR data for **10b** follow. ^{19}F NMR ($PhCF_3$): δ −130.8 (br s). ^{31}P NMR ($PhCF_3$): δ 24.4 (s).

Isolation of 11b. 1b (56.2 mg, 125 μmol) and [(COD)IrCl]$_2$ (41.6 mg, 125 μmol Ir) were mixed in 1 mL of PhF and heated for 2 h at 80 °C. The resultant green solution was filtered through a pad of Celite to remove a minor amount of insolubles, and the volatiles were removed from the filtrate under vacuum. The residue was recrystallized twice from ether/PhF at −35 °C to give 29 mg (35%) of colorless **11b** as a mixture of two diastereomers in a ca. 20:1 ratio. **11b**, major isomer: ^{1}H NMR (C_6D_6): δ 7.29 (m, 1H, Ar−*H*), 7.06−7.14 (m, 2H, Ar−*H*), 6.78−6.86 (m, 2H, Ar−*H*), 6.71 (m, 1H, Ar−*H*), 3.67 (s, 3H, N−*Me*), 3.24 (m, 1H, C*H*Me$_2$), 3.12 (m, 1H, Ir−C*H*aH$_b$), 2.59 (m, 1H, C*H*Me$_2$), 1.65 (m, 2H, C*H*Me$_2$), 1.49 (dd, 3H, J = 8 Hz, J = 15 Hz, CH*Me*$_2$), 1.39 (dd, 3H, J = 7 Hz, J = 15 Hz, CH*Me*$_2$), 0.88−0.96 (m, 6H, CH*Me*$_2$), 0.75 (dd, 3H, J = 7 Hz, J = 16 Hz, CH*Me*$_2$), 0.63 (dd, 3H, J = 7 Hz, J = 16 Hz, CH*Me*$_2$), 0.59 (dd, 3H, J = 7 Hz, J = 17 Hz, CH*Me*$_2$), 0.44 (m, 1H, Ir−CH$_a$*H*$_b$), −21.53 (1H, dd, J = 9 Hz, J = 16 Hz, Ir−*H*). ^{31}P NMR (C_6D_6): δ 32.8 (s), −31.6 (s). ^{19}F NMR (C_6D_6): δ −118.7 (m), −119.0 (m). **11b**, minor isomer: ^{1}H NMR (C_6D_6, selected data): δ −21.27 (1H, dd, J = 9 Hz, J = 16 Hz, Ir−*H*). ^{31}P NMR (C_6D_6): δ 32.0 (s), −39.1 (s). ^{19}F NMR (C_6D_6): δ −117.9 (m), −118.9 (m).

NMR Reaction of 1c/1c-^{13}*C* with [Ir(COD)Cl]$_2$. A J-Young NMR tube was charged with 0.5 mL of C_6D_6, [Ir(COD)Cl]$_2$ (19.4 mg, 0.0576 mmol Ir), and the corresponding ligand (**1c/1c-^{13}*C***, 26 mg, 0.0576 mmol) and shaken well. For the reaction of **1c/1c-^{13}*C*** and [Ir(COD)Cl]$_2$, after 24 h at ambient temperature, the major products are compounds **10c**, **11c**, and **16c** in the ratio of 1:2:1 (plus less than 5% of other minor components). Selected NMR data for **10c/10c-^{13}*C*** follow: ^{1}H NMR (C_6D_6): δ 2.37 (t, J_{H-P} = 6 Hz, Ir−*Me*) for **10c**; 2.37 (dt, J_{H-P} = 6 Hz, J_{C-H} = 138 Hz) for **10c-^{13}*C***. ^{13}C{^{1}H} NMR (C_6D_6): δ −26.4 (t, J_{C-P}= 4 Hz, Ir−*Me*). ^{13}C NMR (C_6D_6): δ −26.4 (qt, J_{C-H} = 138 Hz, J_{C-P} = 4 Hz, Ir−*Me*). ^{31}P NMR (C_6D_6): δ 20−40 (br). Selected NMR data for **11c/11c-^{13}*C*** follow: ^{1}H NMR (C_6D_6): δ 4.41 (s, N−*Me*), −22.6 (dd, J = 9 Hz, J_{C-P} = 17 Hz, Ir−*H*) for **11c**; 4.41 (d, J_{CH} = 140 Hz, N−*Me*), −22.6 (dd, J = 9 Hz, J_{C-P} = 17 Hz, Ir−*H*) for **11c-^{13}*C***. ^{13}C{^{1}H} NMR (C_6D_6): δ 51.4 (s, N−*Me*). ^{13}C NMR (C_6D_6): δ 51.4 (q, J_{C-H} = 138 Hz, N−*Me*). ^{31}P NMR (C_6D_6): δ 38.3(s), −30.9 (s). The ^{31}P NMR resonance at δ −30.9 ppm is a doublet (J_{CP} = 4 Hz) for **11c-^{13}*C***. Selected NMR data for **16c/16c-^{13}*C*** follow: ^{1}H NMR (C_6D_6): δ: 3.78 (t, J_{H-P} = 11 Hz, Ir−C*H*$_2$), −25.7 (t, J_{H-P} = 19 Hz, Ir−*H*) for **16c**; 3.78 (dt, J_{H-P} = 11 Hz, J_{C-H} = 140 Hz, Ir−C*H*$_2$), −25.7 (t, J_{H-P} = 19, Ir−*H*) for **16c-^{13}*C***. ^{13}C{^{1}H} NMR (C_6D_6): δ 17.4 (t, J_{C-P} = 6 Hz, Ir−*C*H$_2$). ^{13}C NMR (C_6D_6): 17.4 (tt, J_{C-P} = 6 Hz, J_{C-H} = 140 Hz). ^{31}P NMR (C_6D_6): δ 28.9 (s).

Isolation of [(^{Me}PN(Me)P)Ir(COD)]$^+$[Cl, (Ir(COD)Cl$_2$)]$^-$ (12a). 1a (35 mg, 0.079 mmol) and [Ir(COD)Cl]$_2$ (26 mg, 0.079 mmol) were placed into a Schlenk flask and treated with 5 mL of toluene. The mixture was stirred for 5 min. The solvent was removed in vacuo, and the residue was washed with pentane, dried under vacuum, and dissolved in CD_2Cl_2 for NMR characterization. NMR data for the [(^{Me}PN(Me)P)Ir(COD)]$^+$ cation follow: ^{1}H NMR (CD_2Cl_2): 7.43 (d, 2H, J = 6 Hz, Ar−*H*), 7.30 (s, 4H, Ar−*H*), 3.88 (s, 3H, N−*Me*), 3.71 (s, 4H, COD), 2.99 (m, 2H, C*H*Me$_2$), 2.40 (s, 6H, Ar−*Me*), 2.26 (d, 4H, J = 10 Hz, COD), 1.76 (d, 4H, J = 10 Hz, COD), 1.68 (m, 2H, C*H*Me$_2$), 1.59 (dd, 6H, J = 7 Hz, J = 14 Hz, CH*Me*$_2$), 1.49 (m, 12H, CH*Me*$_2$), 1.02 (br t, 6H, J = 9 Hz, CH*Me*$_2$). ^{31}P{^{1}H} NMR (CD_2Cl_2): δ 12.8 (s). NMR data for the [Ir(COD)Cl$_2$]$^-$ anion follow: ^{1}H NMR (CD_2Cl_2): 3.74 (s, 4H, COD), 2.11 (m, 4H, COD), 1.28 (m, 4H, COD).

Isolation of [(^{F}PN(Me)P)Ir(COD)]$^+$[Cl, (Ir(COD)Cl$_2$)]$^-$ (12b). 1b (45.0 mg, 100 μmol) and [(COD)IrCl]$_2$ (33.6 mg, 100 μmol) were mixed in 1 mL of fluorobenzene. After 2 h at ambient temperature, the volatiles were removed and the yellow residue was washed with pentane (to remove unreacted **1b**). The residue was recrystallized from CD_2Cl_2/Et_2O at −35 °C. The precipitate was washed with pentane and dried in vacuo to give 40 mg (44% based on **1b**) of **12b** of the composition (as determined by NMR upon dissolution) noted at the end of the paragraph for the elemental analysis. NMR data for the [(^{F}PN(Me)P)Ir(COD)]$^+$ cation follow: ^{1}H NMR (CD_2Cl_2): 7.64 (m, 2H, Ar−*H*), 7.34 (m, 2H, Ar−*H*), 7.31 (m, 2H, Ar−*H*), 4.01 (s, 3H, N−*Me*), 3.75 (br s, 4H, COD), 2.97 (m, 2H, C*H*Me$_2$), 2.29 (br d, 4H, J = 10 Hz, COD), 1.77 (br d, 4H, J = 10 Hz, COD), 1.74 (m, 2H, C*H*Me$_2$), 1.58 (dd, 6H, J_{HH} = 7 Hz, J_{HP} = 14 Hz, CH*Me*$_2$), 1.48 (dd, 6H, J_{HH} = 7 Hz, J_{HP} = 14 Hz, CH*Me*$_2$), 1.46 (dd, 6H, J_{HH} = 7 Hz, J_{HP} = 14 Hz, CH*Me*$_2$), 1.04 (br t, 6H, 9 Hz, CH*Me*$_2$). ^{1}H NMR ((CD$_3$)$_2$CO): δ 7.79 (m, 2H, Ar−*H*), 7.62 (m, 2H, Ar−*H*), 7.42 (m, 2H, Ar−*H*), 4.12 (s, 3H, N−*Me*), 3.88 (br s, 4H, COD), 3.30 (m, 2H, C*H*Me$_2$), 2.38 (br d, 4H, J = 10 Hz, COD), 1.92 (m, 2H, C*H*Me$_2$), 1.82 (br d, 4H, J = 10 Hz, COD), 1.66 (dd, 6H, J_{HH} = 7 Hz, J_{HP} = 14 Hz, CH*Me*$_2$), 1.59 (dd, 6H, J_{HH} = 7 Hz, J_{HP} = 14 Hz, CH*Me*$_2$), 1.54 (dd, 6H, J_{HH} = 7 Hz, J_{HP} = 14 Hz, CH*Me*$_2$), 1.14 (m, 6H, 9 Hz, CH*Me*$_2$). ^{13}C{^{1}H} NMR (CD_2Cl_2): δ 160.8 (dt, J_{CP} = 7 Hz, J_{CF} = 235 Hz, arom. *C*F), 153.8 (t, 10 Hz, arom CN), 137.8 (dd, 30 Hz, 6 Hz, arom. *C*P), 125.9 (t, 8 Hz, arom. *C*H), 119.1 (d, J_{CF} = 22 Hz, arom. *C*H), 118.7 (d, J_{CF} = 23 Hz, arom. *C*H), 64−69 (v br, *C*H of COD), 61.6 (s, N−*C*H$_3$), 32.4 (br s, *C*H$_2$ of COD), 29.3 (d, 19 Hz, *C*HMe$_2$), 26.7 (d, 24 Hz, *C*HMe$_2$), 22.3 (s, CH*Me*$_2$), 21.5 (s, CH*Me*$_2$), 20.4 (d, 6 Hz, CH*Me*$_2$), 19.8 (s, CH*Me*$_2$). ^{31}P{^{1}H} NMR (CD_2Cl_2): δ 13.0 (br s). ^{19}F NMR (CD_2Cl_2): δ −115.7 (br s). NMR data for the [Ir(COD)Cl$_2$]$^-$ anion follow: ^{1}H NMR (CD_2Cl_2): δ 3.74 (br s, 4H, COD), 2.09 (m, 4H, COD), 1.25 (m, 4H, COD). ^{1}H NMR

($(CD_3)_2CO$): δ 3.70 (br d, 4H, COD), 2.05 (m, 4H, COD, overlaps with the solvent peak), 1.21 (app. q, 4H, COD). $^{13}C\{^1H\}$ NMR (CD_2Cl_2): δ 58.7 (s, *C*H of COD), 32.0 (s, *C*H_2 of COD). Anal. Calcd for $C_{33}H_{49}F_2IrNP_2(Cl)_{0.74}(C_8H_{12}IrCl_2)_{0.26}(CD_2Cl_2)_{0.3}$: C, 47.15; H, 5.97; Cl, 7.22. Found: C, 47.12; H, 5.98; Cl, 7.18.

[(^{Me}PN(Me)P)Ir(COD)]$^+$OTf$^-$ (13a). 1a (63 mg, 0.142 mmol) and $[Ir(COD)Cl]_2$ (47.6 mg, 0.142 mmol) were placed into a Schlenk flask and treated with 5 mL of toluene. The mixture was stirred for 5 min, and then Me_3SiOTf (26 μL, 0.142 mmol) was added. The resulting yellow solution was stirred for another 30 min to cause the yellow solid to precipitate. The solid product was collected by filtration followed by washing with toluene. ^1H NMR (CD_2Cl_2): 7.43 (d, 2H, J = 6 Hz, Ar−*H*), 7.28 (s, 4H, Ar−*H*), 3.88 (s, 3H, N−*Me*), 3.71 (s, 4H, COD), 2.99 (m, 2H, C*H*Me$_2$), 2.40 (s, 6H, Ar−*Me*), 2.26 (d, 4H, J = 10 Hz, COD), 1.76 (d, 4H, J = 10 Hz, COD), 1.68 (m, 2H, C*H*Me$_2$), 1.59 (dd, 6H, J = 7 Hz, J = 14 Hz, CH*Me*$_2$), 1.49 (m, 12H, CH*Me*$_2$), 1.02 (vt, 6H, J = 9 Hz, CH*Me*$_2$). The selected ^1H NMR data collected while decoupling the ^{31}P signal at 12.8 ppm follow: 7.28 (s, 2H, Ar−*H*), 1.59 (d, 6H, J = 7 Hz, CH*Me*$_2$), 1.02 (d, 6H, J = 7 Hz, CH*Me*$_2$). $^{13}C\{^1H\}$ NMR (CD_2Cl_2): δ 155.6 (t, 12 Hz, arom CN), 138.0 (s, arom. *C*Me), 135.0 (d, 34 Hz, arom. *C*P), 132.9 (s, arom. *C*H), 132.9 (s, arom. *C*H), 123.1 (d, 6 Hz, arom. *C*H), 63−68 (v br, *C*H of COD), 60.6 (s, N−*C*H$_3$), 32.5 (br s, *C*H_2 of COD), 29.2 (d, 19 Hz, *C*HMe$_2$), 26.5 (d, 24 Hz, *C*HMe$_2$), 22.4 (br s, CH*Me*$_2$), 21.6 (s, CH*Me*$_2$), 20.4 (d, 7 Hz, CH*Me*$_2$), 19.9 (s, CH*Me*$_2$). $^{31}P\{^1H\}$ NMR (CD_2Cl_2): δ 12.8 (s). ^{19}F NMR (CD_2Cl_2): −81.8 (s).

[Bu$_4$N]$^+$[Ir(COD)Cl$_2$]$^-$ (14). CD_2Cl_2 (0.5 mL) was added to $[Ir(COD)Cl]_2$ (20 mg, 0.061 mmol Ir) and $[NBu_4]Cl$ (17 mg, 0.061 mmol) in a J-Young tube. The tube was sealed and shaken well. ^1H NMR (CD_2Cl_2): 3.74 (s, 4H, COD), 3.22 (m, 8H, N−C*H*$_2$), 2.11 (m, 4H, COD), 1.64 (m, 8H, C*H*$_2$CH$_2$CH$_3$), 1.46 (m, 8H, CH$_2$C*H*$_2$CH$_3$), 1.28 (m, 4H, COD), 1.02 (t, 12H, J = 7 Hz, CH$_2$CH$_2$CH$_2$C*H*$_3$).

NMR Reaction of 11c with 1,5-COD. 11c (3 mg) was exposed to air for 1 h and then mixed with 20 μL of 1,5-COD in 0.5 mL of C_6D_6. Solutions of **11c** are stable in the air. After 24 h, no isomerization was observed.

Reaction of [Rh(COD)Cl]$_2$ with 1a-*d*$_3$ or 1c-*d*$_3$. $[Rh(COD)Cl]_2$ (15 mg, 0.062 mmol Rh) was added to a flask containing **1a-*d*$_3$** or **1c-*d*$_3$** (27.7 mg, 0.062 mmol) dissolved in ca. 1 mL of C_6H_6. The flask was heated at 50 °C for 12 h. Then all volatiles were vacuum transferred to an NMR tube. A 3 μL portion of C_6D_6 was added as internal standard. ^2H NMR analysis of the solution resulting from $[Rh(COD)Cl]_2$ and **1c-*d*$_3$** showed incorporation of D in 1,3-cyclooctadiene (^2H NMR: δ 5.84, 5.52, 2.02, 1.33 ppm) found in the volatiles. No detectable ^2H resonances were observed for the volatiles from the reaction of $[Rh(COD)Cl]_2$ and **1a-*d*$_3$**.

Reaction of [Ir(COD)Cl]$_2$ with 1a-*d*$_3$ or 1c-*d*$_3$. $[Ir(COD)Cl]_2$ (20 mg, 0.058 mmol Ir) was added to a flask containing **1a-*d*$_3$** or **1c-*d*$_3$** (26 mg, 0.058 mmol) dissolved in ca. 1 mL of C_6H_6. The flask was stirred at room temperature for 24 h. Then all volatiles were vacuum transferred to an NMR tube. A 3 μL portion of C_6D_6 was added as internal standard. ^2H NMR analysis of the solution resulting from $[Ir(COD)Cl]_2$ and **1c**-d_3 showed incorporation of D in 1,3-cyclooctadiene (^2H NMR: δ 5.84, 5.52, 2.02, 1.33 ppm) found in the volatiles. No detectable ^2H resonances were observed for the volatiles from the reaction of $[Ir(COD)Cl]_2$ and **1a-*d*$_3$**.

Acknowledgment is made to Brandeis University, to Research Corporation, and to the donors of the Petroleum Research Fund, administered by the American Chemical Society, for support of this research. Thanks are expressed to Sara Kunz for assistance with NMR experiments.

Supporting Information Available: Crystallographic information in the form of CIF files, details of synthesis and characterization of compounds **4** and **5**, graphical depiction of the selected NMR data. This material is available via the Internet free of charge at http://pubs.acs.org.

OM050346O